Supplementing White Light with Narrow-Band Light Wavelengths Impacts Cilantro Yield

A Thesis Presented for the

Master of Science

Degree

The University of Tennessee, Knoxville

Colin Gregory Brice

May 2020

ACKNOWLEDGEMENT

Thank you to my parents, Bruce and Debra, and my grandparents for their provisions of encouragement and support during my education. The dedication extends to my loving partner, Kristin, whose tireless patience is truly appreciated.

I want to sincerely thank my major professor, Dr. John Wilkerson, for his close support in the completion of this project. His advice, full of intellect and creativity, is greatly appreciated. My deepest thanks extend to Dr. Neal Eash for bringing me into the Biosystems Engineering and Soil Sciences Department and being a voice of guidance in a new field of study. I especially thank Dr. Forbes Walker and Dr. William Hart for helping support the critical aspects of research and guiding course selections for the term of study.

My special thanks go to Dr. Dean Kopsell, who inspired me to conduct this research and brought me into the world of horticultural research. I want to also thank Dr. John Tyner for helping address many challenges along the way and for imparting an engineer's logic into my work. I am grateful for the academic advising support given by Dr. Daniel Yoder. I would like to also thank Scott Tucker, Jonathan Yoder, Hayden Jordan, and Jordan Brewer for their assistance in the laboratory. I extend my sincere gratitude to David Smith, who was a true friend and took much of his own time to assist in this project.

ABSTRACT

Interest in the use of light-emitting diodes (LEDs) for multilayered, vertical leafy crop production is growing, spurred from increasing demand for energy and resource-efficient food production methods. Researchers built and evaluated a multilayered hydroponic chamber to grow microgreens, a nutrient-dense salad crop. Cilantro (*Coriandrum sativum* L., 'Santo') microgreens were grown in the hydroponic chamber using natural and artificial substrates to determine the impact of substrate on germination rates and fresh yields before conducting LED narrow-band wavelength experiments. The use of artificial foam growth media resulted in higher germination rates than natural fiber substrates (hemp, burlap, coconut) and produced similar fresh yields to burlap (jute fiber).

Light spectra were varied using different narrow-band wavelengths (400 nm, 450 nm, 660 nm, 740 nm) to supplement broad-spectrum white light (3000 K 90 CRI). Fresh shoots were harvested and weighed after 21 days of growth to measure the impact of light wavelength on microgreen yield. Narrow-band red (660 nm) light increased fresh mass (g) per unit energy (kW·h) by 45% over the broad-spectrum white control (3000K 90CRI). Narrow-band blue (450 nm) light increased oven-dried mass by 15% over the experimental control but was not statistically significant ($\alpha = 0.05$).

As seeding rate increased by 40% from 28.5- to 40 g/ 1.7 m² on burlap, fresh mass increased by 80% on average. Broad-spectrum white light supplemented with red light improved fresh yields by 30% and reduced electrical energy usage by 10% compared to the experimental control. An isolated spectrum containing only the four narrow-band wavelengths (400, 450, 660, 740 nm) increased dry mass percentage by 11% compared to the broad-spectrum white control in oven-dried samples. The isolated spectrum increased dry mass content from 8-11% without diminishing yields by a statistically significant amount. Red (660 nm) light supplementation offers a novel tool to increase fresh yields and decrease energy costs simultaneously. The application of blue (450 nm) light and isolated narrow-band light spectra may increase the yields of microgreens dried for production of spices or dietary supplements with longer shelf life.

TABLE OF CONTENTS

CHAPTER 1: INTRODUCTION…..……...……..1

Evolution of Horticulture by Means of Artificial Lighting……...……..1
Research Objectives…...…….…..……..…5

CHAPTER 2: REVIEW OF LITERATURE..…….……..…8
Microgreens……..……..……..……..8
Global Nutrition…...…….…….…….……..……...11
Increasing Dietary Nutrient Intakes...…….…….……13
Vertical Microgreen Production: Nutrient Film Technique Systems…...….....15
Plant Photosystems…....……..……...…..16

CHAPTER 3: DESIGN AND EVALUATION OF A GROWTH CHAMBER FOR MICROGREEN PRODUCTION...….....…21
Introduction……...21
Materials and Methods…….…...……..21
Growth Chamber Construction.…….……..…..23
Air Circulation System……...……...…...…..27
Irrigation Manifold Design …….…….30
LED Assemblies……34
Light Intensity Control …..……..……...…….37
Results and Discussion…….……..……..……..…...…….39
Temperature, Relative Humidity, and Flow Rate……..……...…39
LED Light Uniformity…….....…..……..……...…..43
Electrical Power Usage……..…...44

CHAPTER 4: SELECTION OF SUBSTRATE BY TESTING MEDIA IMPACTS ON CILANTRO GERMINATION RATE AND YIELD.…47
Introduction……...47
Materials and Methods……..……49
Treatments……...……...……...……..52
Statistical Design…….……..……..
Data Collection……...…….……. 57
Analysis…….……..…….58
Results and Discussion……..….....…….....…...59

CHAPTER 5: THE EFFECTS OF SELECT NARROW-BAND LIGHT WAVELENGTHS ON CILANTRO YIELD……..……..65
Introduction…….……..…..65
Materials and Methods…….……..…..65
Treatments…….……..……..……66
Statistical Design…….……..…..70
Data Collection……..……..……70
Analysis…….……71
Results and Discussion…...…….….71
Spectral Measurements of LED Treatments……...72

CHAPTER 6: CONCLUSIONS AND RECOMMENDATIONS……....88

REFERENCES……..……...….90

APPENDIX……..……..……..97

VITA…….……103

LIST OF TABLES

Table 2.1 Phytonutrient content of four microgreen species found to have the highest concentrations (mg/ 100 g fresh mass) of twenty-five varieties tested……..9

Table 2.2 Daily vegetable intakes recommended and sampled by the USDA in 2007-2010……..…….13

Table 3.1 Layout of LED assemblies, showing manufacturer's nominal color and wavelength specifications by treatment (W = broad-spectrum white, IR = infrared, R = red, B = blue, UV = ultraviolet), number of light bars per treatment, and calculated theoretical forward bias voltage (V_f)……...……..……..35

Table 3.2 Temperature values (°C, n = 1) collected from each treatment zone using an Omega type K thermocouple (0.1°C resolution)…….…….40

Table 3.3 Relative humidity (%RH, n = 1) values collected from each treatment zone using a digital hygrometer (1% RH resolution)……41

Table 3.4 Flow rate collected (mL/min) for each irrigation manifold using one-minute collection cycles for calibration……42

Table 3.5 Power usage (W) for each treatment group calculated using measured voltage (V) and current (A), where power = volts * amps. Data is shown alongside calculated forward voltage (V_f)……..……..45

Table 4.1 Treatments used in the germination and yield studies of cilantro (*Coriandrum sativum* var. '*Santo'* L.) split seeds under uniform subirrigation cycles. Commercial artificial substrates tested included both top grooving (TG) and bottom grooving (BG) configurations……...52

Table 4.2 Experimental design of initial germination study of cilantro (*Coriandrum sativum* var. '*Santo"* L.) split seeds under uniform subirrigation cycles (α = 0.05). The logistical regression results are shown beside the table…….……...……56

Table 4.3 Experimental design of second germination study of cilantro (*Coriandrum sativum* var. '*Santo"* L.) split seeds under uniform subirrigation cycles (α = 0.05). The logistical regression results are shown beside the table……58

Table 4.4 Average values for cilantro (*Coriandrium sativum* L. var *'Santo')* microgreen shoot fresh mass (FM) data when grown in controlled environments under different substrate materials with top grooving configuration. Degrees of freedom are shown to the right of the experimental data……..……63

Table 5.1 Treatment layout of final experiments describing position of treatment zones within the cabinet, quantitative color compositions of the treatments, and light wavelength ranges…….67

Table 5.2 Overview of LED experiments, describing sequence, substrate type, and seeding rate. ……..…….…..74

Table 5.3 Average values for cilantro (*Coriandrium sativum* L. var *'Santo')* microgreen shoot fresh mass (FM) and dry mass percentage (%DM) when grown in a controlled environment using 1.25-in. seed cell spacing. Yield-energy ratio is shown for each treatment over the entire crop cycle, calculated using electrical power consumption (W) * cycle length (252 hrs.)……...……....76

Table 5.4 Average values for cilantro (*Coriandrium sativum* L. var *'Santo')* microgreen shoot fresh mass (FM) and dry mass percentage (%DM) when grown in a controlled growth chamber using 1-in. seed cell spacing. Yield-energy ratio is shown for each treatment over the entire crop cycle, calculated using power consumption (W)

and production cycle length (252 hrs.). The logistical regression results are shown below the table……...……..……..79

Table 5.5 Average values for cilantro (*Coriandrium sativum* L. var *'Santo')* microgreen shoot fresh mass (FM) when grown in a controlled growth chamber using burlap. Yield-energy ratio is shown for each treatment over the entire crop cycle, calculated using power consumption (W) and production cycle length (252 hrs.)…...83

Table 5.6 Average values for cilantro (*Coriandrium sativum* L. var *'Santo')* microgreen shoot fresh mass (FM) and dry mass percentage (%DM) when grown in a controlled growth chamber using burlap. Yield-energy ratio is shown for each treatment over the entire crop cycle, calculated using power consumption (W) * cycle length (252 hrs.)……...…….85

LIST OF FIGURES

Figure 1.1 Internal diagram of an LED, showing the circuit assembly, semiconductor chip, and protective casing…….2

Figure 2.1 Diagram of a 7-day old radish (*Brassica oleracea*) microgreen plant. Horizontal lines across the stem show typical cutting locations during harvest……8

Figure 3.1 Shelf and irrigation layout of experimental growth chamber constructed in Spring 2018. Grey circles indicate where irrigation manifolds were inserted into the cabinet wall. Blue arrows illustrate the direction of fluid flow into the treatment zones……...……..……22

Figure 3.2 Irrigation (left) and drain system (right) mounted through sidewalls of experimental growth chamber……...24

Figure 3.3 Close-up view of catch drains (left) and irrigation system (right). Irrigation water passed across the tray surface, through drain holes cut into the tray and mounting assembly, and into a catch-funnel leading to a wastewater tank……..25

Figure 3.4 Close-up view of catch drains (left) and irrigation system (right). Irrigation water passed across the tray surface, through drain holes cut into the tray and mounting assembly, and into a catch-funnel leading to a wastewater tank.…….27

Figure 3.5 A 3-in. PVC ventilation system (right) with six outlets individually connected to each treatment zone…….29

Figure 3.6 A single manifold assembly installed for each of the six treatment shelves……...32

Figure 3.7 Graph displaying the relative emission strength of different-colored LEDs as a function of light wavelength……..36

Figure 3.8 LED wiring assembly showing DIM connections to 10K potentiometers where LED symbols collectively represent a group of light bars in parallel……38

Figure 3.9 Average PAR (*photosynthetically active radiation)* intensity values taken 15 cm beneath each treatment's light array using an Apogee© SP-420 spectrophotometer. Measurements were taken from all six treatment zones and averaged……44

Figure 4.1 Three varying cell spacings of Rootcubes® used in the study……..…..53

Figure 4.2 Illustration of substrate profile view (a) and of grooving placement configurations (b) with top grooving (left) and bottom grooving (right) showing the different seed heights from the water table…….……..54

Figure 4.3 Visual diagram of 100 cm² experimental replicate (above) each containing 2 g of seed and treatment zone (below) shown with ten experimental replicates placed uniformly across each treatment zone. ……...……. 55

Figure 4.4 Germination rates collected during initial substrate material trial using a seeding rate of 0.05 g/cm²…….……..…..59

Figure 4.5 Germination rates collected during substrate configuration study using a seeding rate of 0.05 g/cm²…….……61

Figure 4.6 Fresh cilantro microgreen biomass yields collected during substrate trial using a seeding rate of 28.5 g/1700 cm²……..……..……..63

Figure 5.1 Front view of light treatments, showing six treatment shelves. Each of the six 6800 cm² treatment zones contained four 1700 cm² treatment replicates……...…69

Figure 5.2 Spectral composition and photosynthetic photon flux density (PPFD in μmol·m^{-2}·s^{-1} PAR) by wavelength for narrow-band LED treatments. Relative intensity is shown respective to the most intense wavelength. …….....…73

Figure 5.3 Fresh cilantro microgreen biomass yields collected using 1.25-in. Rootcube® substrate…….……77

Figure 5.4 Oven-dried mass percentages collected during the 1.25-in. Rootcube® trial using a seeding rate of 28.5 g/1700 cm²……77

Figure 5.5 Fresh cilantro microgreen biomass yields collected using 1-in. Rootcube® substrate……80

Figure 5.6 Oven-dried mass percentages collected during the 1-in. Rootcube® trial using a seeding rate of 28.5 g/1700 cm²……..……..80

Figure 5.7 Freeze-dried mass percentages collected during the 1-in. Rootcube® trial using a seeding rate of 28.5 g/1700 cm²……..……..…81

Figure 5.8 Fresh cilantro microgreen biomass yields collected using burlap as a substrate……84

Figure 5.9 Fresh cilantro microgreen biomass yields collected during the burlap trial using a seeding rate of 28.5 g/1700 cm²…….……...86

Figure 5.10 Freeze-dried mass percentages collected during the burlap trial using a seeding rate of 28.5 g/1700 cm²……86

Figure A.1 Photosynthetic photon flux density (μmol·m^{-2}·s^{-1} PAR) by wavelength for the broad-spectrum white LED control group…….…….98

Figure A.2 Photosynthetic photon flux density (μmol·m^{-2}·s^{-1} PAR) by wavelength for the 99% white + infrared supplementation group…….....……99

Figure A.3 Photosynthetic photon flux density (μmol·m^{-2}·s^{-1} PAR) by wavelength for the 40% white + red supplementation group…….……100

Figure A.4 Photosynthetic photon flux density (μmol·m^{-2}·s^{-1} PAR) by wavelength for the 40% white + blue supplementation group. …….……101

Figure A.5 Photosynthetic photon flux density (μmol·m^{-2}·s^{-1} PAR) by wavelength for the 99% white + ultraviolet supplementation group…….…….101

Figure A.6 Photosynthetic photon flux density (μmol·m^{-2}·s^{-1} PAR) by wavelength for the narrow-band isolated spectrum (400, 450, 660, 740 nm) group. Relative intensity is shown respective to the most intense wavelength…….……..102

LIST OF ABBREVIATIONS

B – Blue

CRI – Color rendering index

DM – Dry mass

FM – Fresh mass

HID – High-intensity discharge

IR – Infrared

LED – Light-emitting diode

NFT – Nutrient film technique

PAR – Photosynthetically active radiation

PVC – Polyvinyl chloride

R - Red

SAS- Statistical analysis software

W – White

UV - Ultraviolet

CHAPTER 1: INTRODUCTION

Evolution of Horticulture by Means of Artificial Lighting

Population growth, climate change, and resource scarcity all underline the need for advances in artificial growing systems, including greenhouses, hydroponic production, and vertical gardening. Hemming (2011) describes how growers often use artificial lights to control the light radiation intensity, photoperiod, and spectrum over a crop. Growers use artificial lights under unfavorable light conditions including low light levels, short daylengths, or poor spectral compositions, all of which may impact product quality. Light sources commonly used in horticulture include light-emitting diodes (LEDs), incandescent bulbs, fluorescent tubes, and high intensity discharge bulbs (HID: including high pressure sodium and ceramic metal halide) light technologies. The use of LEDs in a production environment continues to increase as more companies desire the control and potential savings they offer growers.

LEDs consist of a light-emitting electrical circuit encased in a protective cover. Singh et al. (2015) elaborated that LEDs are semiconductors encased in a protective structure that emit light when electrical current is passed through them (Figure 1.1).

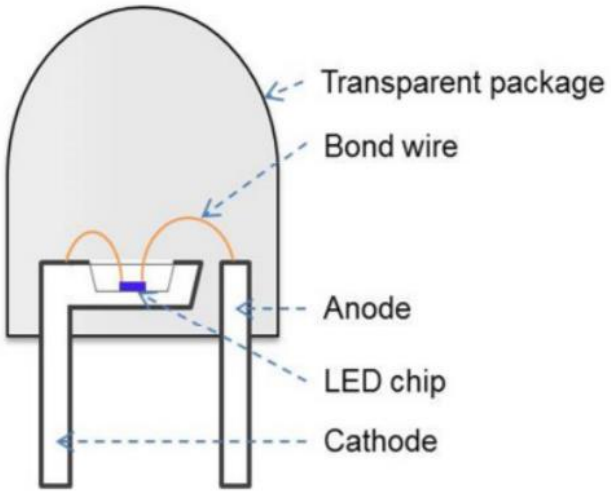


Figure 1.1 Illustration of an LED, showing the circuit assembly, semiconductor chip, and protective casing.

LEDs offer horticultural producers reliable, indoor crop lighting technologies that result in increased energy efficiency. Darko et al. (2014) reported that LEDs produce about 75% less heat per watt compared to incandescent bulbs and convert approximately 80% of electrical energy into photosynthetically active radiation (PAR) or electromagnetic light radiation between the 400-700 nm wavelengths. The authors further noted that HID lamps reached a max fluence of 200 lumens per watt, easily increased ambient temperatures, and prevented mounting lights near the crop canopy. Nelson (2014) described how LEDs emit radiation (light energy) in tightly focused areas, which maximized the radiation transfer to plant leaves in tight indoor spaces. Al-Kodmany (2018) and Despommier (2013) reported that growers can safely place LEDs within a few inches of developing leaf tissue without causing damage or risking a fire.

LEDs can emit narrow bands of light across the spectrum of photosynthetically active radiation (400-700 nm) without the use of filters. Kopsell and Sams (2013) devised a method where LED light may be used to manipulate plant products for desired morphological traits and phytochemical compositions. The authors exposed 13-day old microgreen broccoli (*Brassica oleracea* L., 'Italica') plantlets to red/blue (627/470 ± 5 nm) or blue (470 ± 5 nm) LED light for 5 days before harvest. Kopsell et al. (2017) used a 16-hour photoperiod with 3 different red/blue (627/447 ± 5 nm) LED light ratios to increase fresh yields by 20-50% in Chinese kale (*Brassica oleracea* L., 'Green Lance'). In this study, LED light treatments were applied starting the 15th day of a 30-day growth cycle and resulted in an 83% average increase of total carotenoids compared to the fluorescent/incandescent control. Brazaitytė et al. (2015) reported that it is possible to directly increase the growth rate and nutritional content of microgreens, a juvenile salad crop, using specific light spectra in production systems. LEDs provide horticulturalists new methods to manipulate plant products through the controlled application of certain light wavelengths.

Effects of different narrow-band LED light wavelengths on crop phytonutrient content have been characterized in some studies. Kopsell and Sams (2013) exposed sprouting broccoli (*Brassica oleracea* L., 'Italica') to blue LED light (470 nm) and red/blue LED light (627/470 nm) treatments which resulted in statistically-increased levels of beta-carotene, violaxanthin, xanthophyll cycle pigments, glucoraphanin, epiprogoitrin, and aliphatic glucosinolates. Essential micronutrients also increased significantly; This increase included copper, iron, boron, manganese, molybdenum,

sodium, zinc, and essential macronutrients of calcium, phosphorus, potassium, magnesium, and sulfur.

Samuolienė et al. (2017) grew microgreens of mustard (*Brassica juncea* L., 'Red Lion'), beet (*Beta vulgaris* L., 'Bull's Blood'), and parsley (*Petroselinum crispum* Mill., 'French') under five sole-source LED configurations. Each consisted of four narrow spectral bands: 638 nm red + 660 nm red + 731 nm infrared + 445 nm blue. The authors concluded that carotenoid and xanthophyll concentrations may be directly manipulated to higher levels using moderate (16-33%) blue light concentrations. Metabolite increases were concluded to be solely influenced by light treatment which displayed effects of varying magnitude between the tested species. The authors varied blue (445 nm) light levels from from 0% (control), 8%, 16%, 25%, and 33% relative to the total light intensity at 250 $\mu mol \cdot m^{-2} \cdot s^{-1}$ PAR. Concentrations of chlorophylls A and B and certain carotenoids (alpha- and beta-carotenes, lutein, violaxanthin, and zeaxanthin) were found to be 1.2 to 4.3 times higher under 33% blue light relative to lower blue light concentrations. Accumulation of metabolites not scientifically connected with light reactions (xanthophylls) took place under 16% blue (445 nm) light, increasing 1.3 times that of the control.

Hammock (2018) found that in hydroponically grown basil (*Ocimum basilicum* L., 'Genovese'), a red-blue ratio of 60:40 resulted in significantly increased total fresh weight, macronutrients, micronutrients, and volatile organic compounds using red (627 nm) and blue (447 nm) supplemental wavelengths. This hydroponic

study of basil utilized a 60:40 red-blue ratio for light supplemented to broad spectrum sunlight. As growers expand the use of artificial lighting strategies, application methods must be engineered to optimize the photosynthetic conversion of light radiation into crop growth. Controlled light applications using LEDs may offer more productive methods of producing nutritious foods in malnourished regions of the world. Kyriacou et al. (2017) stated that future space exploration and colonization requires adequate food supplies with minimal resupply from Earth. The authors urged scientists and growers to develop strategies for producing whole-food sources of vitamins and minerals. They further noted that microgreens are an ideal crop candidate for this type of research, due to their adaptability to indoor environments and high nutrient density.

Research Objectives

As the adoption rate of artificial lighting in horticultural production increases, new light application strategies are required to minimize energy costs in commercial production systems. This research focused on determining how different narrow-band light wavelengths influence cilantro (*Coriandrum sativum* L., ‘Santo’) fresh and dry biomass yields. There are few studies with a novel system design approach to microgreen production in general or that pertain to the effects of light wavelength on cilantro. A gap exists in the literature regarding studies that explore light application strategies to increase the rate of plant growth while minimizing light energy input. *Coriandrum sativum* provides not one, but two staple culinary ingredients (cilantro

and coriander seed) and is an extremely popular herb. There is a pronounced lack of information available on hydroponic production of cilantro in nutrient film technique hydroponics. This research advanced vertical microgreen production technologies by illustrating novel ventilation, irrigation, and LED lighting system design concepts that increased the energy efficiency and biomass production of a vertical, hydroponic cilantro production system.

Researchers developed and evaluated an indoor, hydroponic chamber to maintain abiotic factors (temperature, relative humidity, light intensity, and irrigation) across six treatment zones. Several substrate materials, thicknesses, and seed densities were tested under the designed irrigation system. Substrates that resulted in higher germination rates of cilantro (*Coriandrum sativum* L., 'Santo') were tested to measure which substrates resulted in higher fresh cilantro microgreen biomass. Substrates that performed better in both germination and yield tests were used to grow cilantro microgreens under different LED light treatments for fresh and dry biomass weight analysis. Four LED treatments supplemented white LED light with a different narrow band light wavelength (Ultraviolet: 400 ± 5 nm, blue: 450 ± 5 nm, red: 660 ± 5 nm, and infrared: 740 ± 5 nm). A fifth treatment consisted only of the four narrow band light wavelengths and did not contain a broad spectrum. Broad spectrum white light was used alone as a control. Researchers compared fresh and dry harvested biomass of cilantro grown under different narrow-band light wavelengths used to supplement white LED light. All shoot and leaf tissue were harvested and weighed from four replicates on the 21st day after sowing for fresh and dry biomass data collection.

The research was focused on the following objectives:

- Design, develop, and evaluate a vertical hydroponic chamber to maintain environmental conditions between experimental light treatments. The system was evaluated on its ability limit variation between treatment areas by measuring temperature, relative humidity, and volumetric flow rate.

- Compare performance of natural and synthetic substrate materials on cilantro microgreen germination rate and yield (g).

- Evaluate impact of four narrow band LED light wavelengths (ultraviolet: 400 nm, blue: 450 nm, red: 660 nm, and infrared: 740 nm) on cilantro microgreen biomass (g) when used to supplement white light (410-780 nm).

CHAPTER 2: REVIEW OF LITERATURE

Microgreens

Microgreens, a specialty salad crop, are gaining popularity for their nutritional content and aesthetic quality. It was noted by Xiao et al. (2012) that chefs incorporate microgreens into their cuisine as a garnish, as they possess strong flavors and aesthetically improve most dishes. Treadwell and Hochmuth (2017) state that any edible plant that can be harvested at or before the first true leaf stage can be produced as a microgreen. The roots are not eaten due to their contact with the growing media which can leave inedible debris in the root hairs. Xiao et al. (2015) further define microgreens as the fleshy foliage and hypocotyl of a seedling plant (Figure 2.1).

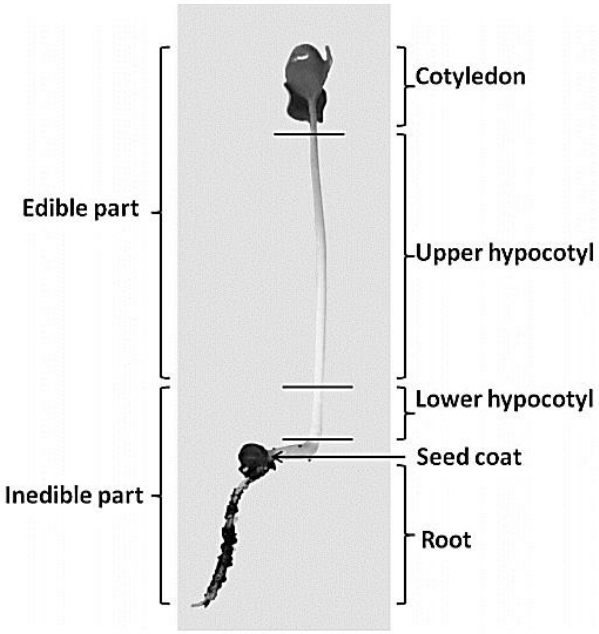


Figure 2.1 Illustration of a 7-day old radish (*Brassica oleracea*) microgreen plant. Horizontal lines across the stem show typical cutting locations during harvest.

Due to the general demand for strong flavor, herbs and spicy greens are often grown and sold as microgreens. Kyriacou (2016) found that the *Brassicaceae, Asteraceae, Chenopodiaceae, Lamiaceae, Apiaceae, Amarillydaceae, Amaranthceae, Fabaceae, and Cucurbitaceae* families are often grown in microgreen systems for their simple germination and cultivation requirements, seed availability, and short crop cycle (7-10 days). Other examples of commonly grown microgreens include cilantro (*Coriandrium sativum* L.), basil (*Ocimum basilicum* L.), dill (*Anethum graveolens* L.), sunflower (*Helianthus annuus* L.), radish (*Raphanus sativus* L.), and pea (*Pisum sativum* L.). Producers can produce dozens of species as microgreens, but typically will produce a select few varieties for which there is current local demand.

Microgreens contain numerous phytochemicals that are important to human health. Xiao et al. (2012) described the approximately 3-inch-tall crop as juvenile greens or herbs with high phytonutrient densities. Their results, synopsized in Table 2.1, demonstrated that levels of several phytonutrients range from 5 to 40 times that of the same mature plant species.

Table 2.1 Phytonutrient content of four microgreen species found to have the highest concentrations (mg/ 100 g fresh mass; FM) of twenty-five varieties tested.

mg/ 100 g FM	Red cabbage (*Brassica oleracea* L., '*capitata'*)	Cilantro (*Coriandrum sativum* L.)	Garnet amaranth (*Amaranthus hypochondriacus* L.)	Green daikon radish (*Raphanus sativus* L., '*longipinnatus'*)
Ascorbic acid	147.0	40.6	131.6	70.7
β-carotene	11.5	11.7	8.6	6.1
Phylloquinone	0.28	0.25	0.41	0.19
α-tocopherol	24.1	53.0	17.1	87.4

In the study of twenty-five microgreen varieties, red cabbage (*Brassica oleracea* L., '*capitata'*), cilantro (*Coriandrum sativum* L.), garnet amaranth (*Amaranthus hypochondriacus* L.), and green daikon radish (*Raphanus sativus* L., '*longipinnatus')* possessed the highest levels of ascorbic acids (provitamin C), carotenoids (provitamin A, lutein, zeaxanthin), phylloquinone (provitamin K), and tocopherols (provitamin E), respectively. Cilantro microgreens contained higher levels of beta-carotene, lutein/zeaxanthin, and violaxanthin than most other species.

Kopsell and Sams (2013) noted that many human health benefits are attributed to physiological carotenoid activity. Kopsell and Kopsell (2006) define carotenoids as yellow, orange or red pigments that are found in many vegetable crops and which comprise an important class of phytochemicals. They elaborate that beta-carotene serves as the precursor to vitamin A in mammalian systems. Kopsell and Sams (2013) describe the antioxidant activity of carotenoids in scavenging free-radicals, suppressing cancer development, enhancing immune-response, and protecting eye tissues. Samuolienė (2017) describes the consumption of carotenoids and other phenolic compounds as being linked to antioxidant and anticarcinogenic activity in the human body. Darko et al. (2014) state that reactive oxygen species harm cellular proteins and nucleic acids, but that they are covalently bound or "quenched" by plant antioxidants. Darko et al. (2014) further noted that carotenoids offer a wide range of health benefits, play an important role in health, and should be prioritized in a healthy diet.

Global Nutrition

Ahmed et al. (2018) described malnutrition as both over- and undernutrition, where malnutrition is usually only thought of as undernutrition. Malnutrition was described to include both nutrient deficiencies and excesses which can result from genetic or environmental factors, such as predisposition to diabetes or poor diet. Undernutrition refers to a diet containing inadequate amounts of calories, protein, or micronutrients required for sound growth. Martins (2011) reported that malnutrition can impair physical and neurological development and lead to disease, impaired growth development, and death. Martins (2011) estimated that half of all deaths in children under five were associated with malnutrition. Others (Onis et al., 2011; Walker et al., 2007) argue that malnutrition also causes anxiety, antisocial behavior, oppositional disorder and is associated with violence and crime. Naber (1997) studied a sample of 155 patients, 70 mild to severely malnourished patients showed 70% greater odds of having a gastrointestinal disease than those deemed well-nourished by Subjective Global Assessment standards. Test subjects had limitations and needed assistance with personal hygiene and eating, due to disease and age. On a societal level, disease prevalence is partly caused by inadequate intake of nutrients needed to maintain and protect organ systems.

Biswas (1986) reported that many people in countries where corn is a staple crop were undernourished. Cediel et al. (2015) noted that corn and beans, common staple crops, lack many essential vitamins, and minerals necessary for proper

development. Huang et al. (2006) suggested undernourishment is somewhat attributable to the fact that traditional corn *(Zea mays)* varieties lack adequate levels of lysine and tryptophan. Lysine and tryptophan are two essential dietary amino acids needed to form proteins in the human body. Therefore, improper nutrition places a notable handicap on society, leading to preventable disease and impairing the development of humankind. Countries with staple crops lacking in essential nutrients must explore methods of supplemental nutrition to ensure proper dietary intakes.

Personal choice plays an important role in determining a person's lifespan and disease susceptibility. Willett (2002) affirmed that environmental factors such as diet and lifestyle are more important than genetic factors in causing avoidable diseases. The author pragmatically argued a balanced approach that focused on factors which may be more easily changed. Doll and Peto (1981) estimated that 35% of cancer deaths in the United States were possibly avoidable by dietary modification. The National Cancer Institute (2011) reported that between 2007 and 2010, 75-86% of Americans did not meet USDA intake recommendations with over half receiving less than two servings of fruit and three servings of vegetables daily. The USDA (2010) guidelines for a 2,000-Cal diet recommended most people eat at least four daily servings of both vegetables and fruit, shown in Table 2.2.

Table 2.2 Daily vegetable intakes recommended and sampled by the USDA in 2007-2010.

	Daily Servings (0.5 cup equivalent) by Varying Caloric Requirements						
Food Group	**1,200 Cal**	**1,400 Cal**	**1,600 Cal**	**1,800 Cal**	**2,000 Cal**	**Actual Serving Sizes**	**Serving Contents (g)**
Recommended Vegetable Intake	3.5	3.5	3.5	4.5	4.5	1 cup raw leafy vegetable or 0.5 cup chopped	33.5
Average Vegetable Intake	1.5	1.5	1.5	1.5	1.5	1 cup raw leafy vegetable or 0.5 cup chopped	33.5
Average Dark-Green Vegetable Intake	0.1	0.1	0.1	0.1	0.1	1 cup raw leafy vegetable or 0.5 cup chopped	33.5
Recommended Fruit intake	3.5	4	4	4.5	4.5	1 medium fruit	100
Average Fruit Intake	1.1	1.1	1.1	1.1	1.1	1 medium fruit	100

Table 2.2 shows a pronounced lack of vegetable intake in the average American diet. Americans are eating less than half of the recommended amount of vegetables. To meet dietary guidelines, Americans must start consuming twice as many vegetables or consume similar amounts of vegetables which are twice as nutrient-dense.

Increasing Dietary Nutrient Intakes

Pragmatic cultural change can be made through the introduction and spread of crop production techniques which had previously undiscovered values. The

improvement of a food or crop's nutritional value may impart dietary benefits to a population. Bouis and Saltzman (2017) defined biofortification as a method of increasing a crop's vitamin and nutrient density using plant breeding, transgenics techniques, or agricultural practices. The authors stated that Nicaragua, Panama, and Cuba have integrated biofortification into their national food security agendas, and Guatemala is progressing in its evaluation and propagation of promising biofortified crops.

Biofortification of staple crops (corn, beans, etc.) has shown some recent success, where between 2007 and 2015, 29 biofortified seed varieties were released to farmers in Latin American countries for agricultural production. Semilla Nueva (2017), a research organization working in Guatemala, introduced quality-protein corn, which contains double the amount of lysine as regular corn varieties. Nuss and Tanumihardjo (2011) reported that quality protein maize can meet dietary protein requirements at intake levels 40% lower than normal maize. The authors also described the increased content of lysine (from 265 mg to 408 mg/100 g) and tryptophan (from 67 mg to 75 mg/100 g) in common and quality protein maize. Biofortified seed has been distributed to over 24,000 individuals with 12.5 metric tons being released in 2017. Research is playing an important role in shaping how organizations fight malnutrition across the world. Crop biofortification can improve a population's nutritional intake, but more research emphasis should be placed on developing methods to increase production of nutritious foods containing a broad range of phytonutrients.

Vertical Microgreen Production: Nutrient Film Technique Systems

Nutrient film technique (NFT) allows the consistent indoor production of high-density vegetable crops, especially leafy herbs, vegetables, and microgreens. NFT is a hydroponic method of crop production where plants have their roots in a shallow layer of recirculating water containing all dissolved plant nutrients. Cooper (1996) describes NFT as a method where well-drained substrate is needed only to anchor the plant. The mass of the root system lies across the water "film" surface, allowing access to both oxygen and nutrient-rich water. Resh (2012) synopsizes the early development of nutrient film hydroponics and names Cooper a pioneer of the method. The author mentioned that most commercial NFT systems are currently used to produce leafy greens and herbs. Resh (2012) noted that Dr. P.A. Schippers modified the NFT technique in 1977 to include a vertically stacked, cascading pipe system which was displayed at Disney's Epcot. The author reported Schippers' goal was to reduce the greenhouse space needed to grow a given number of plants and reduce the cost per plant, and eventually focused on low-growing crops, including lettuce. Microgreens are approximately 3-in. tall crops which are well-adapted to vertical hydroponic production systems.

Vertical microgreen systems should be regularly sanitized to prevent contamination. Microgreen products may pose risks to consumers, however, if systems are not cleaned and sanitized regularly. Xiao et al. (2015) state that *Escherichia coli* may proliferate within hydroponic microgreen systems. Short production cycles (5-21

days), allow more frequent sanitation of hydroponic systems than longer crop cycles would allow. Kaiser and Ernst (2018) discuss how *Pythium* and *Phytophthora* fungi are common pathogens to an NFT crop and *Aphidoidea* and *Thysanoptera* insects are also known to infest NFT systems. Regular sanitation and microbial contact prevention are especially important factors to consider when producing microgreens hydroponically. Therefore, microbial exposure must be managed and prevented in hydroponic microgreen production.

Indoor NFT crops have complex requirements for the substrate, as the substrate must foster proper water, nutrient, and oxygen availability. From the work of Metallo (2017), it was shown how microgreen production can depend on species genetics, but abiotic factors such as temperature, relative humidity, water, substrate, light intensity, and light wavelength also affect plant growth. Resh (2012) described substrate factors for plants grown in NFT systems. Rockwool and other manufactured substrates (e.g Oasis Rootcubes®) are popular in NFT hydroponics due to their uniform wettability and porosity. Substrates are designed to allow control of saturation, fertility, and aeration while providing structural support to the plant. These environmental factors, especially temperature, relative humidity, water, substrate, light intensity, and light wavelength play essential roles in promoting a healthy crop.

Plant Photosystems

In controlled indoor production settings, light becomes a factor of increased importance due to the reduction or total elimination of solar radiation. Hemming

(2011) reported that in commercial horticulture, high-pressure sodium lamps are often used to provide even radiation levels across growth areas, but they result in excessive thermal load to the environment relative to LEDs. Cummings et al. (2007) noted that this increases the operating cost of cooling and dehumidification systems. Conversely, increasing temperatures lowers relative humidity which may impact plant growth through effects on transpiration. Indoors, light fixtures which give off more heat increase the risk of fire, encouraging indoor growers to use LEDs or fluorescent fixtures.

Understanding the basics of plant physiology is important when selecting artificial lights for indoor production. Taiz et al. (2015) described how light-harvesting antennae within the plant perform the light reactions of photosynthesis and provide chemical energy for the assimilation of carbon dioxide into sugars. The authors explained that light in the 625-700 nm wavelength region is absorbed most efficiently by photosystem antennae complexes within the chloroplast. Darko et al. (2014) reported that the indoor production market abundantly uses the application of white light with individual wavelength supplementations. This is done to increase growth rate, stimulate flowering, or manipulate other forms of crop physiology.

Individual wavelengths of light may be supplemented to a broad spectrum for improved plant growth. Several studies (Samuolienė, 2017; Kopsell and Sams, 2013; and Kopsell et al., 2017) have demonstrated specific effects of narrow-band light wavelengths. Red light (630-660 nm) can be supplemented or added to broad spectrum

light to increase photosynthetic activity at high absorption levels. Blue light (450 nm) enhances levels of carotenoids and volatile organic compounds across several microgreen species. Broad spectrum white light, however, may be solely used to grow plants indoors because its light spectrum resembles that of natural sunlight.

In the absence of broad-spectrum light, microgreens develop mutated growth characteristics. In growth chambers and vertical farms, plants can be grown in the absence of infrared or “far-red” light (700 nm-1 mm) resulting in small leaves and stems. Runkle (2016) reported the effects of far-red radiation on plant growth. The author described infrared light as an essential environmental signal necessary to promote healthy biochemical pathways within the plant. Although undetectable by the human eye, infrared light is known to impact plant growth by its influence on the phytochrome pigment. Li et al. (2011) discussed how the ratio of red to infrared light controls the interchangeable conversion of phytochrome into two forms: red-absorbing and far-red absorbing. Increased far-red to red light ratios promote the formation of the far-red absorbing form of phytochrome, which promotes stem and leaf expansion and can control flowering. While infrared light may not efficiently conduct photosynthesis, it has notable impact on the development of stems and leaves.

Ultraviolet (UV) light has peculiar effects on plants. White and Jahnke (2002) mentioned how UV-A light (320-400 nm) has been shown to lower photosynthetic activity while increasing beta-carotene concentration in two species of algae. Szymanska and Slezak (2017) found that under short, acute light and temperature

stress, antioxidant levels seem to increase within plants. Stapleton (1992) noted that ultraviolet light in the UV-C (200 to 280 nm) and UV-B (280 to 320 nm) regions has been shown to cause severe damage to plant systems. Damage was described in two forms of damage, first being to DNA and second being to physiological cellular processes and systems. Darko et al. (2014) concluded that excess light radiation not utilized by the plant stresses the plant and results in increased reactive oxygen species formation, harming cellular proteins and nucleic acids. While some forms of ultraviolet light (UV-B and UV-C) are apparently lethal to plants, UV-A light plays a synergistic role in the formation of nutritionally beneficial compounds, but not in stimulating photosynthesis.

Ramankutty et al. (2008) remarked that, globally, 40% of ice-free land is being used for agriculture to feed the growing population. Foley (2005) blamed agricultural intensification for environmental concerns such as tropical deforestation, biodiversity loss, habitat loss, greenhouse gas emissions, soil quality losses through erosion and salinization, decreases in water resource quantity and quality, alteration of regional climates, leaching of fertilizers, and reduction in air quality. Earth's population approaches eight billion people, many of which live in cities. Despommier (2013) described the Green Revolution, when agricultural advances removed food as a limiting factor to human population growth through improved grain yields and crop breeding strategies. Food production is tasked to expand and meet the needs of the growing population that will exceed 10 billion in a few decades, but direct expansion of current agricultural systems may limit resources and land for the future.

As climate change and resource scarcity become limiting factors to population growth, technologies are needed to increase yield productivity per unit area. Houghton (2003) and Defries and Achard (2002) estimated that the clearing of forest for grazing and cultivation causes approximately 12-26% of total carbon dioxide emissions in the atmosphere through microbial degradation. Yang et al. (2003) discussed how in the last century, the development of new farms and grazing lands has caused an accelerated rate of soil erosion, which may be increased by global warming. Khoo and Knorr (2014) alongside others (Myers et al., 2013) described a scientific obligation in developing reliable production methods for more abundant production of nutritious crops using fewer resources. Increasing food production under traditional agricultural models adds to the instability of soil, climate, and water quality. Societal factors place pressure on growers to incite another green revolution, and growers must investigate new ways to become more productive using less space and energy.

CHAPTER 3: DESIGN AND EVALUATION OF A GROWTH CHAMBER FOR MICROGREEN PRODUCTION

Introduction

LEDs used in this research had low electrical usage and heat production relative to incandescent/florescent lighting technologies. Light-emitting diodes contain light emitter circuits encased in a water-resistant cover which allowed safe operation within 5 inches of the crop canopy. LED wavelength experiments used a controlled environment growth chamber built to hydroponically produce cilantro under maintained environmental conditions. Growth conditions were maintained to allow tested factors (substrate and light wavelength) to solely impact the crop across treatment zones. The chamber limited variations in irrigation, temperature, relative humidity, and light intensity between the treatment zones to reduce experimental error. Six vertically-stacked growth trays (1.2 m x 0.61 m) each contained four treatment zones (0.51 m x 0.25 m) used to conduct the experiments discussed in chapters 3, 4, and 5.

Materials and Methods

A vertical, hydroponic growth chamber was designed in the Sensors and Controls Lab at The University of Tennessee. The chamber was constructed to grow microgreens on six shelves (Figure 3.1).

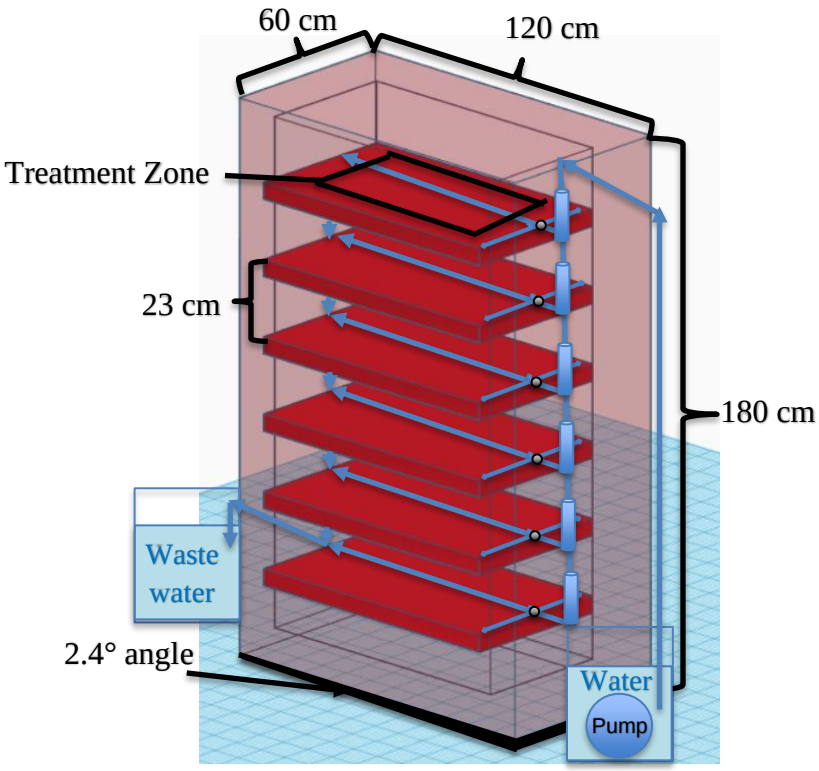


Figure 3.1 Shelf and irrigation layout of experimental growth chamber constructed in Spring 2018. Grey circles indicate where irrigation manifolds were inserted into the cabinet wall. Blue arrows illustrate the direction of fluid flow into the treatment zones.

Growth Chamber Construction

An industrial, steel storage cabinet (1.22 m x 0.61 m x 1.83 m) was modified into a vertical hydroponic growth chamber (Figure 3.2). The cabinet was positioned to one side at an approximate 2.4° horizontal angle (5 cm height over 120 cm length) to allow drainage across six hydroponic trays spaced 23 cm apart. The six plastic trays were mounted inside the cabinet to minimize ambient light within the treatment zones. Manifolds were connected using 1-in. reinforced vinyl tubing. Six drains filled a catch tank which was emptied between experiments. A sliding drawer assembly allowed easy removal of shelves from the cabinet to streamline harvest and subsequent sanitization.

Drawer slides were bolted through the cabinet wall into a free hanging PVC baseboard, atop of which the trays rested (Figure 3.3). Hydroponic shelves were transported to a harvest table and placed into an industrial sink for sanitization. Interior cabinet surfaces were sanitized with a 10% w/v Clorox® bleach and water solution between crops. Shelves were removed and scrubbed with the diluted bleach solution to remove contaminants and reduce the risk of crop disease and contamination.



Figure 3.2 Irrigation (left) and drain system (right) mounted through sidewalls of experimental growth chamber.



Figure 3.3 Trays (left) and sliding drawer/irrigation system (right) mounted into the experimental growth chamber. Hydroponic trays rested atop sliding boards mounted to the cabinet sidewall. Drains were inserted into the ends of the trays, which transferred fluid through the sliding board and into a catch-drain.

The steel industrial storage cabinet was converted into a hydroponic growth chamber with automated lighting and irrigation. Six metal shelves (1.22 m x 0.610 m) were removed and replaced with polyvinyl chloride (PVC) sliding trays that attached to 0.550 m drawer slide mounts. PVC trays were cut from ceiling panels (1.22 m x 0.610 m; 6 mm thickness) and trim board (2.4 m x 0.08 m; 25 mm thickness) purchased from Home Depot®.

Trays were adhered using a plastic cement and sealed using caulking. Aluminum angle (91 cm x 0.6 cm x 3.8 cm; 3 mm thickness) was bolted into the underside of the tray frame to prevent distortion, which would have resulted in uneven water distribution (Figure 3.4). A 9 mm hose barb was placed into a hole drilled at the left side of the tray irrigation surface, allowing drainage from the shelf. The baseboards were drilled with 10 mm holes to allow transfer of fluid through the slide tray assembly. Foam rings were attached at the point of contact between the tray and the baseboard to minimize leaking. Catch drains were inserted through 21 mm holes cut into the cabinet wall opposite to the supply piping. The drain was not connected to the tray, but, instead, “floated” below the baseboard, allowing fluid transfer and full usage of the sliding trays.



Figure 3.4 Close-up view of catch drains (left) and irrigation system (right). Irrigation water passed across the tray surface, through drain holes cut into the tray and mounting assembly, and into a catch-funnel leading to a wastewater tank.

Air Circulation System

The ventilation system minimized variability of temperature and relative humidity between the treatment zones. The growth areas were supplied with ambient air surrounding the growth chamber. The treatment zones were continuously maintained to a similar temperature and humidity as the air surrounding the ventilation intake. The cabinet's total air volume was replaced continuously with surrounding room-temperature air. The air velocity within each treatment zone was below detectable levels, but nominal calculations were used to size the fan for a selected nominal air velocity of 0.3 m/sec.

Given:

Nominal air velocity = 0.3 m/sec

Treatment zone length = 1.22 m

Treatment zone width = 0.610 m

Treatment zone height = 0.230 m

$$\frac{0.3\ \text{m}}{\text{sec}} * \frac{0.610\ \text{m}}{\text{width}} * \frac{0.23\ \text{m}}{\text{height}} * \frac{60\ \text{sec}}{1\text{-min}} = \frac{2.5\ \text{m}^3}{\text{min}}$$

The fan was oversized by 10% at a nominal flow rate of 2.8 m^3/min to allow adequate air cycling rates for the whole cabinet, calculated below.

$$\frac{1\ \text{min}}{2.8\ \text{m}^3} * \frac{1.36\ \text{m}^3}{\text{cabinet}} * \frac{60\ \text{sec}}{1\text{-min}} = \frac{29\ \text{seconds}}{\text{cabinet}}$$

Using a fan with 2.8 m^3/min capacity in an enclosed 1.36 m^3 volume cycled the total cabinet volume with fresh air approximately every 29 seconds. A 3.5-in. inline turbine fan (TerraBloom®, USA) with a nominal flow rate of 2.8 m^3/min rated at 18 W was attached to the air intake and operated continuously. The ventilation system consisted of 3-in. PVC piping, tees, and 4-in. aluminum ducting (Figure 3.5). The intake was connected to six outlets, which inserted into 8.8 cm holes cut in the side of each treatment zone. The system was constructed from 3-in. tees and PVC pipe, which inserted into the sidewall of each treatment zone.

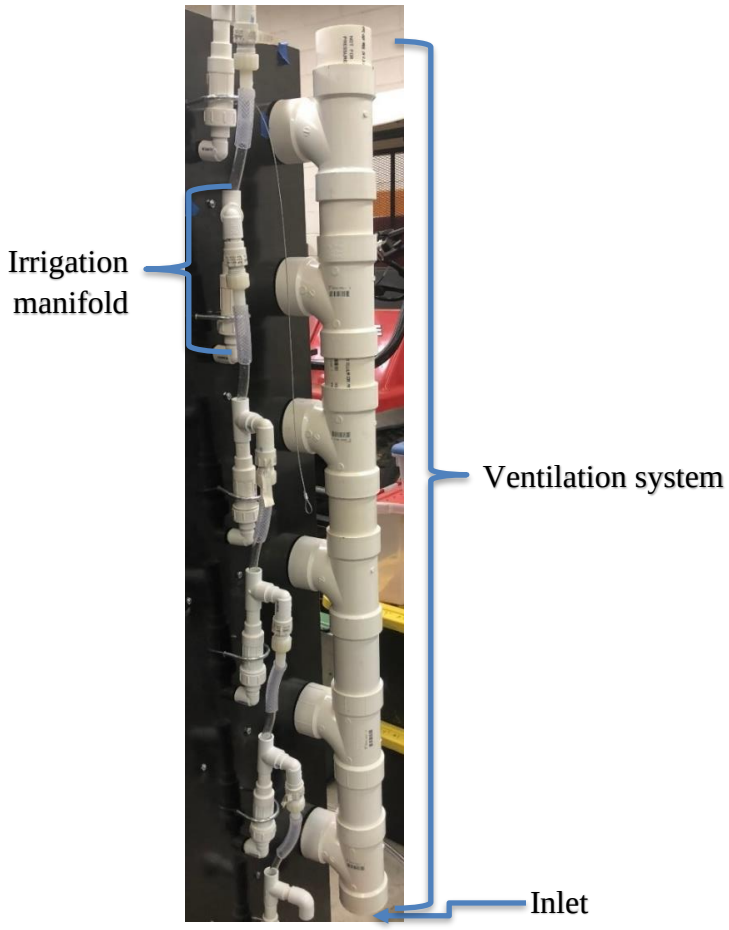


Figure 3.5 A 3-in. PVC ventilation system (right) with six outlets individually connected to each treatment zone.

Irrigation Manifold Design

Hydroponic trays were irrigated through a PVC pipe system supplied from a 0.375-in. vinyl plastic hose connected to an aquarium pump which supplied irrigation across the tray surface. A novel irrigation manifold was designed with the purpose of dispensing equal flow rates of water across each treatment zone. Manifolds were constructed from 0.5-in. adjustable PVC couplings connected to a 0.75-in./0.5-in. reducer tee and a 0.5-in. pipe manifold with endcaps.

Overflow and fill tubes of consecutive manifolds connected to 0.75-in. reinforced vinyl-plastic tubing. Flow rate was maintained through the manifold design itself, where simple hand-extension of the adjustable coupling allows the grower to make minor manual-adjustments (±2.3% of full range) to flow rate. Hand adjustment was used to reduce variability below 5%. This was done to prevent the interaction of irrigation factors with substrate and light wavelength treatments. Irrigation manifolds contained stainless-steel filters (No. 50 woven mesh size) inserted within the threaded connection of the adjustable coupling. This limited pathogens from reaching the crop and reduced risk of a clogged irrigation orifice (1.5 mm diameter).

Manifolds were filled with water from an overhanging pipe connected to a timed pump. Flow rates were selected based on the volume of the thickest substrates tested. Irrigation flow rate was sized to provide 25% of the thickest substrate volume which ensured excess would drain from the thinner substrates. Thicker foam substrates

(1 cm thickness) resulted in a total substrate volume of 5000 mL per shelf. Thinner fibrous substrates (approximately 0.3 cm thickness) resulted in a total substrate volume of 1300 mL per shelf. To allow even air/water ratios on the root surface, manifolds were designed to provide 25% volumetric water content to the substrates. Fibrous substrates required 325 mL per irrigation event while thicker foam substrates required 1250 mL per irrigation event. The average of the two volumes, 780 mL was used to size the irrigation flow rate for an anticipated one-minute irrigation cycle. Watering manifolds maintained a constant head pressure dependent on the height of the adjustable coupling (Figure 3.6).

Water filled in the upper manifold opening and distributed evenly across the two halves of the manifold boom to equalize flow rate across the surface of the first treatment zone (tray). Water then filled the manifold chamber, whose height was determined by the adjustable coupling setting. This caused an overflow which transferred fluid to the subsequent manifold's fill tube through the reinforced tubing.

Manifold chambers overflowed and transferred water downwards to the next manifold in series by gravity. Manifolds were vented to the atmosphere, so orifical pressure is determined by vertical height (h) or "head" between overflow tube and orifice. Several calculations were performed using given manifold height and expected number of orifices (6) to determine orifice size for a desired flow rate (780 mL/min).

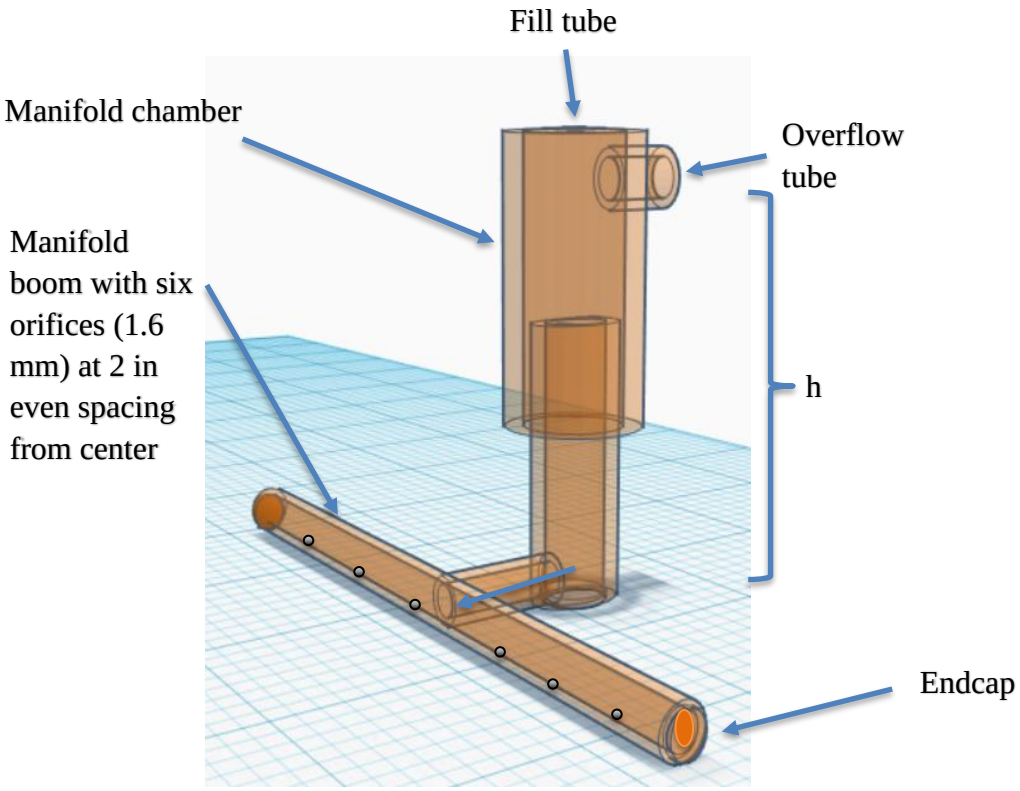


Figure 3.6 A single manifold assembly installed for each of the six treatment shelves.

Adjustable manifold coupling possessed a variable overflow tube height of 12-20 cm with an interior rubber O-ring seal. An average of the height ranges (16 cm) was used to determine the size of orifices using the orifice flow equation.

$$Q = CA\sqrt{2gh}$$

Where: Q = flow rate (mL or cm^3/sec)

C = orifice constant (0.61)

A = orifice cross-sectional area

g = gravitational acceleration constant (980 cm/s^2)

h = vertical head (cm)

Given: Q = 780 mL/min (for all six orifices)

h = 16 cm

Find: Diameter (cm) for a single orifice

Solve:

$$cm^2 = \frac{130\ cm^3/sec}{(0.61)(2)(980\ cm/s^2)(16\ cm)} = 0.067\ cm^2$$

To find diameter (cm), using area of circle equation ($A = (\pi d^2)/4$)

$cm = \sqrt{(4)(0.067\ cm^2)}/4 =$ <u>0.13 cm</u> or approximately 1 mm drill bit size

All six watering manifolds handled fluid in the same manner but there was a delay between subsequent manifolds “priming” and transferring fluid to the next in

series. Manifold chamber volume and transfer tube length caused a slight delay in fluid priming of watering manifolds over the course of the 1-min irrigation cycle.

Hand adjustments were made to the adjustable coupling to compensate for this nominal variation caused by the priming delay. The final design provided a flow rate or 870 mL/min on average which exceeded the desired nominal flow rate of 780 mL/min by 11.5%.

LED Assemblies

A total of 22 LED light bars were each adhered to a 1-in. aluminum channel using double-sided, heat resistant tape. Holes were drilled into the sides of the channel, to allow the insertion of a small, 8-32 machine screw. This screw attached to a chain, which was used to hang several light bars 15 cm over each treatment zone (Table 3.1).The upper five treatment shelves each contained two white LED bars placed above the crop, perpendicular to the length of the shelf. The lower five shelves each contained colored light bars oriented perpendicular to the shelf length. LEDs mounted on linear printed circuit boards were selected for specified emission wavelength peaks (Cutter Electronics©, Australia).

Table 3.1 Layout of LED assemblies, showing manufacturer's nominal color and wavelength specifications by treatment (W = broad-spectrum white, IR = infrared, R = red, B = blue, UV = ultraviolet), number of light bars per treatment, and calculated theoretical forward bias voltage (V_f).

Treatment	Light bar color and wavelength (±10 nm)	# of LEDs in series	Forward bias voltage per diode (V_f)	Forward voltage per light bar (V_f)
W	White (410 – 780 nm)	16	3.4	54.4
99W1IR	White (410 – 780 nm)	16	3.4	54.4
	IR (740 nm)	6	1.9	11.4
40W60R	White (410 – 780 nm)	16	3.4	54.4
	Red (660 nm)	15	2.1	31.5
60W40B	White (410 – 780 nm)	16	3.4	54.4
	Blue (450 nm)	6	3.1	18.6
99W1UV	White (410 – 780 nm)	16	3.4	54.4
	UV (400 nm)	6	3.5	21
1IR 59R 39B 1UV	IR (740 nm)	6	1.9	11.4
	Red (660 nm)	15	2.1	31.5
	Blue (450 nm)	6	3.1	18.6
	UV (400 nm)	6	3.5	21

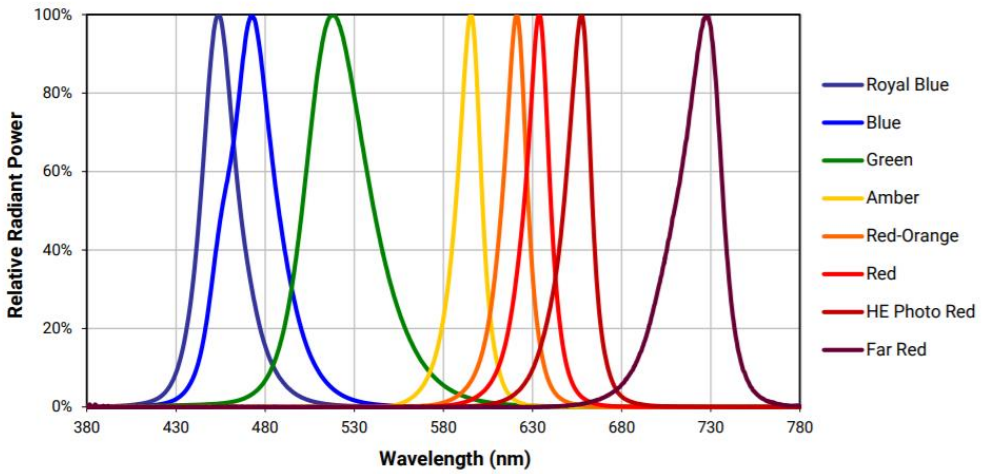


Figure 3.7 Graph displaying the relative emission strength of different-colored LEDs as a function of light wavelength.

Bandwidths of the LEDs vary based upon color, but relative radiant power (W/m^2) and luminous flux (lumens) decay rapidly for wavelengths (±10 nm) surrounding the peak. XP-E and XP-E-2 LED's were used for red, infrared, blue, and white light (product codes XPEEPR-L1-0000-00C01, XPEFAR-L1-0000-00701, XPEROY-L1-0000-00B02, and JB3030AWT-00-0000-000A0UC435E, respectively); (Cree©, Durham, UT, USA). UV light was supplied using specialized emitters (product code C3535U- UNL1-A1G11H-U50); (ILS©, United Kingdom). Direct current power drivers (Meanwell©, Taiwan) were specified based on calculated forward voltages of each light bar (Table 3.1) and used to power individual LED light bar circuits. The numbers of light bars in parallel were used to size LED driver amperage ratings, which were manufacturer specified at 350-1000mA. Stranded-core wire (18 AWG) was used to connect the lights to the LED drivers. Driver output voltages were at 12-V, 20-V, 24-V, 36-V, and 54-V for the infrared (740 nm),

ultraviolet (400 nm), blue (450 nm), red (660 nm), and white (410-780 nm) light bars, respectively.

Light Intensity Control

Hydroponic trays each contained a treatment zone (6800 cm^2) split into four 1700 cm^2 treatment areas. Trays were vertically spaced 23 cm apart. Each treatment zone was photo-isolated, meaning light could not pass between any of the six treatment zones. Treatment zones were split into four replicate areas, totaling four replications per treatment. Lights levels were measured on dark shelves adjacent to illuminated shelves using a NIST-traceable calibrated spectrophotometer (model SP-420, Apogee Instruments©, Logan, UT, USA). Rootcube (Smithers-Oasis©, Kent, OH, USA) and burlap (Burlapper©, USA) substrates were placed on the shelf surface and the cabinet doors were closed before taking readings to simulate the experimental conditions. Light radiation was not detected below the shelf in which LEDs were being operated. Therefore, each of the six treatment zones were exposed to LED light spectra contained to each zone.

A control panel was built and installed to control light intensity for each LED driver. Alternating current power (120V @ 60 Hz) was diverted through a series of nine double-pole single-throw switches. Each switch had on and off controls to each LED driver. One set of terminal blocks was used to make a joined connection to individual switches.

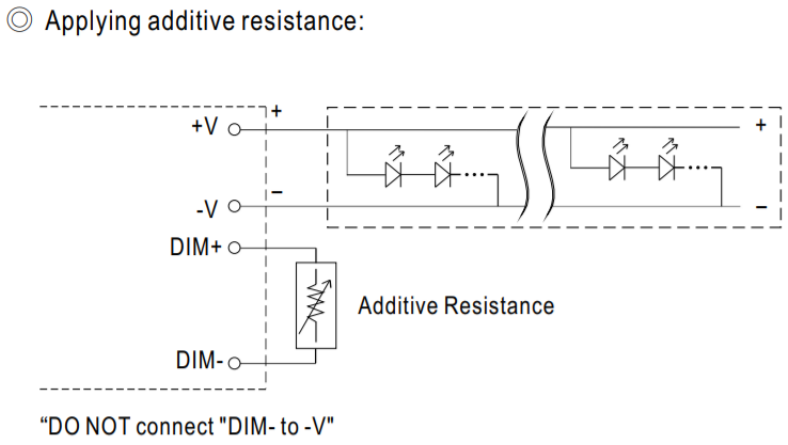


Figure 3.8 LED wiring assembly showing DIM connections to 10K potentiometers where LED symbols collectively represent a group of light bars in parallel.

Each switching circuit was then isolated through a set of terminal blocks that connected to the input of the LED drivers. Potentiometers (10K) were connected to the DIM+ output control circuit for each LED power driver. Wiring assembly is shown in Figure 3.8 The SP-420 spectrophotometer was used to calibrate each treatment's color spectrum. Therefore, each treatment zone containing white lights had an individual control circuit for its white LED bars and its colored LED bars. Light spectrum calibration occurred by adjusting each white and individually colored light circuit on each shelf to the percentage values shown in Table 3.1 on page 28. For the control, the white lights were set at 250 $\mu mol \cdot m^{-2} \cdot s^{-1}$ PAR. For the second treatment, infrared intensity was set to 1% of 250 $\mu mol \cdot m^{-2} \cdot s^{-1}$ PAR light intensity while the adjacent lights were turned off. The same procedure was performed to the other lights where percentage of total intensity was measured while adjacent lights were not being powered. Output control by use of potentiometers successfully allowed calibration of

light intensities to exact values specified by the treatment levels with a precision of ±1 $\mu mol \cdot m^{-2} \cdot s^{-1}$ PAR.

Results and Discussion

Many horticultural studies are conducted in greenhouse bays, which can experience severe fluctuations in temperature and relative humidity across a single season, potentially interacting with treatments across a single crop cycle. The growth chamber's purpose was to maintain uniformity of temperature, relative humidity, irrigation, and light intensity between treatment and zones to reduce their impact on crop growth. The system was evaluated on its ability to maintain environmental conditions within a 10% coefficient of variation by measuring temperature, relative humidity, and volumetric flow rate.

Temperature, Relative Humidity, and Flow Rate

The ventilation system's purpose was to maintain uniform temperature and relative humidity between treatment zones. Temperature and relative humidity were measured during each set of experiment to monitor variation during crop growth. Temperature values varied between ±3.3 °C across treatment shelves on any given sampling date (Table 3.2),

Table 3.2 Temperature values (°C, n = 1) collected from each treatment zone using an Omega type K thermocouple (0.1°C resolution).

Shelf #	10/15/2018 T °C	11/6/2018 T °C	1/4/2019 T °C	2/14/2019 T °C	4/19/2019 T °C	CV %
1	21.9	19.3	21.1	17.8	20.3	7.96%
2	21.5	19.0	22.5	17.5	19.0	10.3%
3	21.1	19.6	21.2	17.2	19.5	8.22%
4	20.9	19.8	20.9	16.9	18.7	8.68%
5	20.5	19.9	20.1	16.7	18.5	8.14%
6	20.3	20.3	20.0	16.1	16.7	11.2%
CV	2.86%	2.34%	4.33%	3.56%	6.43%	

Cabinet doors were closed for 5 minutes prior to each reading. Readings were taking briefly during each experiment to ensure environmental factors were maintained. The ventilation-system maintained temperature between treatment zones below a coefficient of 6.43%. Temperatures varied more throughout different sampling dates to a maximum of 11.2%. Relative humidity values were maintained within a 10% coefficient variation (Table 3.3).

Cabinet doors were closed for 5 minutes prior to each reading. Readings were taking briefly during each experiment to ensure environmental factors were maintained.

Table 3.3 Relative humidity (%RH, n = 1) values collected from each treatment zone using a digital hygrometer (1% RH resolution).

Shelf #	10/15/2018 %RH	11/6/2018 %RH	1/4/2019 %RH	2/14/2019 %RH	4/19/2019 %RH	CV %
1	48%	53%	40%	33%	47%	17.6%
2	49%	51%	46%	32%	51%	17.4%
3	46%	53%	42%	33%	49%	17.1%
4	47%	52%	42%	34%	47%	15.3%
5	46%	51%	46%	32%	47%	16.3%
6	48%	53%	47%	32%	44%	17.5%
CV %	2.56%	1.88%	6.52%	2.50%	4.94%	

Relative humidity was maintained within a 6.52% coefficient of variation across treatment zones. Humidity varied by more than 15% due to seasonal effects but was kept uniform between the treatment zones using the ventilation system. The research ventilation system caused less variation between the treatment zones on a given date than there was surrounding the chamber on different sampling dates. This is likely due to the fluctuating atmospheric temperature and relative humidity from changing seasons or even simple adjustments to air conditioning settings by university staff. The static plumbing system was designed to provide equal flow rates to six trays at different elevations using a small aquarium pump. The plumbing system was calibrated using one-minute volumetric calibration procedures to limit variation in irrigation flow rate between each treatment zone. Half-inch PVC adjustable couplings

were used as manifold chambers to allow minor nominal adjustments to flow rate. Data from three calibration events are shown in Table 3.4. Flow rate exceeded the desired flow rate of 780 mL/min by 11.5%. The six manifolds ultimately maintained a near-uniform average flow rates across each shelf with a 0.96% coefficient of variation. Flow uniformity varied by over 5% in initial calibration events.

The absolute range of flow rates achieved by hand-adjustment from the final manifold design was 40 mL or ±2.3%, ranging from 850-890 mL. Three manifolds were added after two calibration events for final system assembly. The irrigation pump was powered for one minute and water volume was collected and transferred into a 2-L graduated cylinder. Table values are the average volumes of three, one-minute cycles.

Table 3.4 Flow rate collected (mL/min) for each irrigation manifold using one-minute collection cycles for calibration.

Shelf #	**6/20/2018* mL/min**	**6/28/2018* mL/min**	**10/15/2018 mL/min**
1	616	400	850
2	530	357	850
3	541	350	855
4*	-	-	865
5*	-	-	855
6*	-	-	870
CV %	8.32%	7.34%	0.958%

The small aquarium pump (VicTsing©, USA) initially used had a 300 LPH flow rate rated at 4 W and required 10 seconds to prime only three prototype manifolds, causing 7-8% variation over a planned one-minute irrigation cycle. Extensive design modifications reduced the fluid charging delay between subsequent manifolds. The manifold was completely redesigned to fill more quickly by reducing the chamber volume and height. The water pump ultimately selected was a 1550 LPH 25 W submersible pump (Homasy©, USA) which allowed a 2-3 second priming process and provided adequate flow rate to quickly charge all six of the water manifolds against a head of 2 m. After the two redesign processes, the design resulted in flow variation under 1% between the treatment zones.

LED Light Uniformity

LED manufacturer's viewing angle specifications were used to space light assemblies adjacent to each other and reduced the variability of light intensity across the treatment zones. The 120° angle at which 50% intensity occurred was used to set spacing with an expected 15 cm emitter distance from the leaf canopy. Light intensity was measured using an Apogee© spectrophotometer positioned directly underneath a single light bar. Light was measured 15 cm from the light emitter at the expected crop canopy height (5-7 cm). Average measurements from each treatment zone was used to determine light variation in a 20 cm width. A 10 cm sampling zone width was used to collect freeze-dried and oven-dried plant tissue samples. Light intensity readings are shown in Figure 3.9.

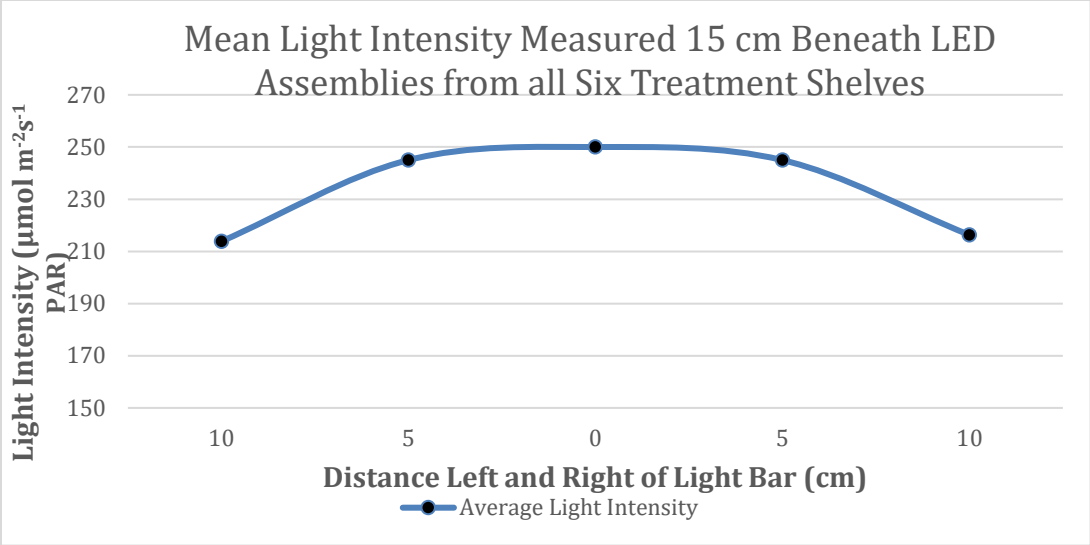


Figure 3.9 Average PAR (*photosynthetically active radiation)* intensity values taken 15 cm beneath each treatment's light array using an Apogee© SP-420 spectrophotometer. Measurements were taken from all six treatment zones and averaged.

Electrical Power Usage

Power consumption of each LED treatment was calculated using voltage (V) and current (A) measured with a precision digital voltmeter (BK©, USA; precision: 1 mA, 1 mV). Power was calculated using measured voltage to derive total energy usage for comparing yields under different light treatments. By creating a ratio between fresh harvested biomass (g) and energy usage (kW·h), a meaningful term is created that correlates the productivity of the system to its energy usage. The measured values were used to calculate power usage for each treatment zone, shown in Table 3.5.

Table 3.5 Power usage (W) for each treatment group calculated using measured voltage (V) and current (A), where power = volts * amps. Data is shown alongside calculated forward voltage (V_f).

Treatment	Light bar color and wavelength (±10 nm)	Measured DC Voltage (V)	Measured DC Current (A)	Power per light bar (W)	Power per treatment (W)
W	White (410-780 nm)	44.0	0.316	13.9	27.8
99W1IR	White (410-780 nm)	43.2	0.247	10.7	25.0
	IR (740 nm)	12.0	0.300	3.60	
40W60R	White (410-780 nm)	42.0	0.097	4.07	24.9
	Red (660 nm)	27.7	0.303	8.39	
60W40B	White (410-780 nm)	42.8	0.183	7.83	24.3
	Blue (450 nm)	17.6	0.246	4.33	
99W1UV	White(410-780 nm)	44.0	0.303	13.3	27.9
	UV (400 nm)	18.5	0.034	0.629	
1IR 59R 39B 1UV	IR (740 nm)	12.0	0.300	3.60	30.3
	Red (660 nm)	27.7	0.303	8.39	
	Blue (450 nm)	17.6	0.246	4.32	
	UV (400 nm)	18.5	0.034	0.620	

The table above shows that manufacturer specifications were appropriately used to size the LED drivers, where measured forward voltages were near manufacturer's reported forward voltages. The lower values are likely due to manufacturer specifications being given for operation at 350 mA, where all light bars were operated below 320 mA. The narrow-band spectrum consumed the most power, while the narrow-band blue treatment used the least amount of power.

The results demonstrate the various energy requirements for each light treatment group. These results allow comparison of yield for each light treatment based upon the measured power consumption.

CHAPTER 4: SELECTION OF SUBSTRATE BY TESTING MEDIA IMPACTS ON CILANTRO GERMINATION RATE AND YIELD

Introduction

"Germination" is described by Bewley and Black (1985) as a commonly misunderstood process where the term is often used loosely. Germination begins when a seed imbibes water and ends when the embryonic axis, usually the radicle, starts to elongate. Dead seeds can imbibe water but will not successfully germinate and produce a visible radicle. The elongation and protrusion of the radicle is caused by a series of biochemical events (protein hydration, cellular structure rearrangement, respiration, cellular elongation, and macromolecule formation).

The International Seed Testing Association (2020) issues guidelines for seed health testing procedures and sampling guidelines, which ensure standard procedure when testing the healthy or consumer safety of seeds. These guidelines primarily deal with ensuring health of seed, referring to the presence of disease-causing organisms, animal pests, and trace element deficiencies. This research took a systems approach, and, instead, sought to determine how germination is affected by substrate under the uniform irrigation cycle discussed in the previous chapter. This approach was taken to determine a substrate that would result in higher germination rates and fresh yields before conducting further experiments with LED light treatments.

Seed germination is a major factor influencing production success in hydroponics, especially in microgreen systems. Microgreen production in NFT hydroponics can be streamlined by the ability to germinate and grow microgreens to maturity in the same area without transporting substrate or trays. Bewley and Black (1985) also mention that seed germination can be hindered by the presence of light, so growers often germinate seeds in total darkness before placing them under lights for vegetative growth. The hydroponic growth chamber used maintained darkness during germination before lighting cycles were initiated the 9^{th} day.

The irrigation system supplied 870 ± 20 mL of water to each treatment area once per day during the experiments. This was performed to simulate production using the static plumbing system, which was designed to restrict water usage and to operate using a single pump. The germination studies tested the ability of commonly used hydroponic substrates (Rootcubes®, Horticubes®, jute fiber, coconut fiber pad, and hemp fiber pads) to germinate seeds under a continuous NFT irrigation cycle. Yan (2016) mentions that coconut fiber has high lignin content and is made in the same process as jute fiber. The raw materials are steeped in hot water before fibers are removed from the plants by brushing. The cellulose and lignin content of the fibers help determine their physical characteristics, which impact hydrophobicity.

Materials and Methods

Open-pollinated, untreated cilantro (*Coriandrum sativum* L. var. '*Santo*') split seeds were obtained from Johnny's® Seeds company in January 2018 and stored dry at 4.4°C for nine months during construction of the growth chamber. Seeds were stored to simulate regular aging from storage during commercial production. Seeds were germinated in the prototype vertical growth chamber under uniform environmental conditions. Two germination studies and one yield trial used different substrates to grow cilantro microgreens and determine effects of substrate type on germination rates and fresh yields in NFT hydroponics.

Differences in substrate, not irrigation water, impacted germination and subsequent yields. Substrate water holding capacity and porosity are hypothesized as critical factors in the water management scheme. The interaction of irrigation method, substrate material, and substrate properties impacted the germination and yield of cilantro (*Coriandrum sativum* L., 'Santo). In the first germination study, three types of natural substrate were tested against three artificial substrates under uniform NFT irrigation cycles across the same area. NFT irrigation cycles lasted 1 minute every 24 hours, calibrated to deliver 850-890 mL of water per day across each of six 6800 cm^2 treatment zones. Cycles only occurred once per day to simulate a commercial production where automated irrigation is not feasible. Darkness was maintained except during the collection of germination, temperature, and relative humidity data. Fertility or other nutrients were not added to the irrigation water.

The second germination test compared five artificial substrates of the same material, but with varying size configurations. Our leading hypothesis was that cilantro germination rate will increase using thinner substrates which more readily imbibe water. A yield trial was conducted following the two germination experiments using the five substrates that resulted in the highest modeled germination probabilities. To determine a final substrate for use in the LED wavelength experiments, yield was analyzed under the five substrates that resulted in higher germination rates and yields in the first two studies. Substrates materials and configurations that demonstrated the highest germination rates and yields were subsequently used in the light wavelength studies.

Kretschmer (1978), Covell et al. (1986), and Metallo (2017) discussed that temperature, relative humidity, and irrigation factors could impact rate and success of seed germination. Therefore, temperature, relative humidity, and light intensity were maintained throughout the growth chamber for the duration of the three studies to prevent interaction with treatment factors. Temperature was held between 19-23°C and was measured using a handheld digital thermometer. Relative humidity was maintained between 40-53%.

Treatments

To test a variety of substrates, three natural substrates were tested including burlap (jute fiber), coconut fiber pad, and hemp fiber pads. Tests were performed to

determine the performance of substrates in the prototype system based on physical characteristics and a limited watering cycle. Paper towel tests were not performed to determine original viability of the seed. Hydroponic media were evaluated in their ability to germinate seeds by comparing germination rates collected 9 days after sowing. All treatments were exposed to 3500 Kelvin broad-spectrum white LEDs (Cree®, Durham, NC, USA) with a color rendering index of 90 (CRI).

Treatments received 250 $\mu mol \cdot m^{-2} \cdot s^{-1}$ PAR for 12 continuous hours each day starting the seventh day after sowing until harvest on the 21st day. There were approximately 50 seeds to a gram and seeds were approximately 4-5 mm in diameter. A seeding rate of 28.5 g/1700 cm^2 replicate zone was used with roughly 1,425 plants per treatment.

Table 4.1 Treatments used in the germination and yield studies of cilantro (*Coriandrum sativum* var. '*Santo'* L.) split seeds under uniform subirrigation cycles. Commercial artificial substrates tested included both top grooving (TG) and bottom grooving (BG) configurations.

	Treatments					
Shelf number	1	2	3	4	5	6
Experiment 1: germination by substrate material	1.5-in. Rootcubes ® (TG)	1.25-in. Rootcubes® (TG)	1-in. Rootcubes ® (TG)	Hemp Fiber	Jute fiber (burlap)	Coconut fiber
Experiment 2: germination by substrate configuration	1.5-in. Horticube ® XL (TG)	T2 – 1.5-in. Horticube® XL (BG)	T3 – 1.25-in. Horticube ® XL (TG)	T4 – 1.25-in. Horticube ® XL (BG)	T5 - 1-in. Horticube ® XL (TG)	T6 – 1-in. Horticube® XL (BG)
Experiment 3: fresh yield substrate trial	1.5-in. Rootcube ® (TG)	1.25-in. Rootcube® (TG)	1.5-in. Horticube ® XL (TG)	1.25-in. Horticube ® XL (TG)	1-in. Horticube ® XL (TG)	*

A sixth treatment was not used in the yield study due to the lack of LED fixtures which emitted white light in the sixth treatment area. Darkness was maintained during germination. During the yield trial, all treatments were exposed to 3500K 90CRI broad-spectrum white LED light starting the ninth day after sowing, receiving 250 $\mu mol \cdot m^{-2} \cdot s^{-1}$ PAR with a 12-hour photoperiod. Treatments replicates received 850-890 mL of water every 24 hours until germination rates were taken on the ninth day. Yields were harvested on the 21st day from substrates which resulted in higher germination rates. Initial substrate test focused on material, which determined

germination rate by the material's ability to absorb and hold water over a 24-hour period with a regular watering schedule.

Once material was tested, substrate configuration was varied across treatment zones to determine impact of substrate configuration on germination rate. Three seed-cell spacing configurations of synthetic-plastic Smithers-Oasis Rootcubes® were tested, shown in Figure 4.1. Top performing substrates were used in the substrate yield trial before beginning the light wavelength experiments. Rootcube® and Horticube® materials are made from phenolic foams and possess relatively low cation exchange properties. The foams are engineered to provide ideal water to air ratios to the plant root. Seeds were sown into grooves (seed-cells) cut into the surface of rooting material to allow roots some mechanical leverage in penetrating the foam-like material. The length, width, and height of grooves cut into substrate were identical. Varying seed-cell spacing changed seed density at a given seeding rate for a given area of substrate material.



1-in. Medium **1.25-in. Medium** **1.5-in. Medium**

Figure 4.1 Three varying cell spacings of Rootcubes® used in the study.

To determine if substrate configuration had an impact on germination success, seeds were germinated in a second experiment atop six different configurations of Smithers-Oasis Horticubes®, a different foam-like material than was used in the previous study. For each of three size configurations, both top and bottom grooving configurations were tested, as shown in Figure 4.2.The two grooving types result in different height of the seed bed relative to the water table. Bottom grooving configuration exposed seeds to light and elevated them by 1 cm. Top grooving options protect the seeds from nearby light and place them closer to a restricted water table. Top grooving configurations were hypothesized to result in higher germination rates compared to bottom grooving. Artificial substrates' seed-cell spacing configurations impacted seeding rate and air volume within the developing leaf canopy (Figure 4.2).

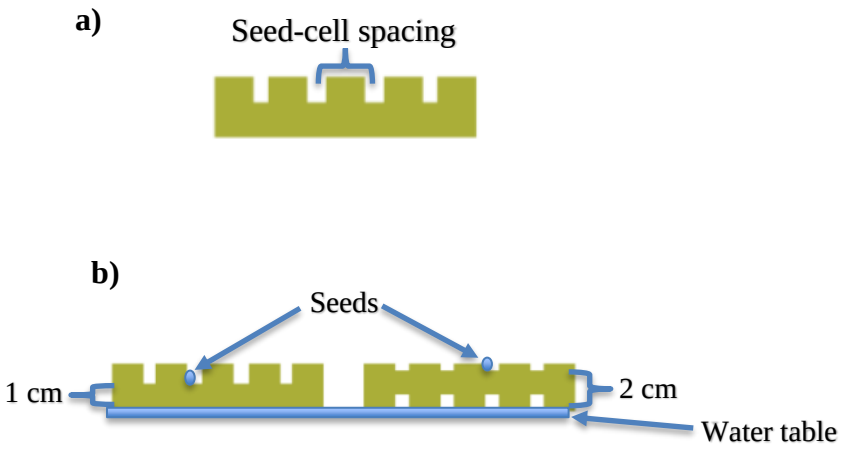


Figure 4.2 Illustration of substrate profile view (a) and of grooving placement configurations (b) with top grooving (left) and bottom grooving (right) showing the different seed heights from the water table.

Statistical Design

The studies employed a randomized design in a controlled vertical growth chamber. Cilantro seeds were randomly placed on tested substrate treatments in groups of equal mass (2g) in both germination studies. Small treatment pieces (10 cm x10 cm) were placed across the treatment zone to simulate several replications under the same environmental conditions. The experimental layout of a treatment zone is represented in Figure 4.3. Each shelf comprised a single treatment zone filled with a single substrate type. Ten treatment replicates were evenly placed across each treatment zone in the first study. Twenty treatment replicates were evenly placed across each treatment zone in the second germination study.

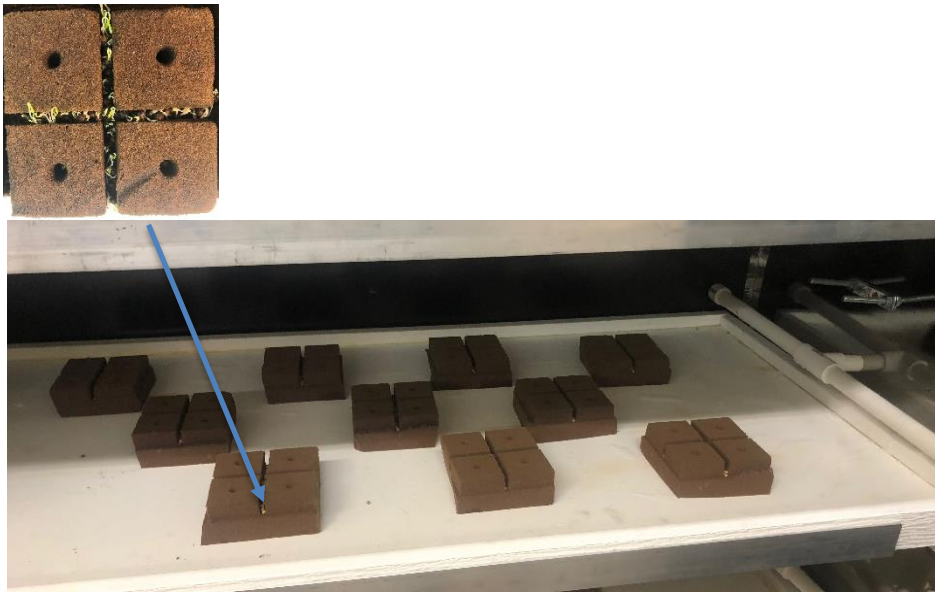


Figure 4.3 Visual diagram of 100 cm^2 experimental replicate (above) each containing 2 g of seed and treatment zone (below) shown with ten experimental replicates placed uniformly across each treatment zone.

Four 1700 cm² treatment replicates were placed on each treatment zone in the yield trial. Tukey's mean separation test was conducted on yield data to test fixed effects based on location across the shelf with no statistically significant effects at the 95% confidence level (Table 4.2). Logistical regression procedures did not allow for mean separation tests to be performed on germination data. Darkness was maintained during germination until 60 seeds were counted from each treatment replicate. Treatments replicates received 850-890 mL of water every 24 hours until germination rates were taken on the ninth day. Substrate treatments were applied to ten treatment replicates per each of six-1700 cm² treatment zones, totaling 3,600 sampled seeds.

Table 4.2 Experimental design of initial germination study of cilantro (*Coriandrum sativum* var. '*Santo"* L.) split seeds under uniform subirrigation cycles (α = 0.05). The logistical regression results are shown beside the table.

Substrate treatment	**Replicates per treatment**	**Seeds sampled per replicate**
1-in. Rootcube®	10	60
1.25-in. Rootcube®	10	60
1.5-in. Rootcube®	10	60
Hemp	10	60
Burlap	10	60
Coconut	10	60
Total	**60**	**3600**

Type III Tests of Fixed Effects				
Effect	Num DF	Den DF	F Value	Pr > F
treatment	5	54	26.40	<.0001

Data Collection

Seeds were the sampling unit, where 60 seeds were sampled from each replicate under a given substrate treatment. Bewley and Black (1985) describe visual germination as the point at which the radicle becomes visible as it emerges from the seed coat. Following the research methods of Behdarvandi (2014), individual seeds were recorded as either “germinated” or “not germinated” (scored by visible 1 mm radicle protrusion). To increase sample size relative to methods by Tarquis and Bradford (1992) and others (Covell et al., 1986; Diouf et al., 2015), germination rates were calculated by scoring 60 seeds uniformly sampled from all sides of each treatment replicate.

Following the methods of Kopsell and Sams (2013), fresh shoots were harvested from a 1700 cm^2 treatment replicate and the fresh shoot mass recorded in the yield trial. Recorded fresh mass was collected as fresh yield by cutting all above-ground plant material (stems and leaves). Darkness was maintained during germination until 60 seeds were counted from each treatment replicate on the ninth day. Treatments replicates received 850-890 mL of water every 24 hours until germination rates were collected. Six substrate treatments (DF = 5) were applied to twenty treatment replicates per each of six-1700 cm^2 treatment zone, totaling 7,200 sampled seeds.

Table 4.3 Experimental design of second germination study of cilantro (*Coriandrum sativum* var. '*Santo"* L.) split seeds under uniform subirrigation cycles (α = 0.05). The logistical regression results are shown beside the table.

Substrate Treatment	Replicates per treatment	Seeds sampled per replicate
T1- 1.5-in. Horticube® XL (TG)	20	60
T2 – 1.5-in. Horticube® XL (BG)	20	60
T3 – 1.25-in. Horticube® XL (TG)	20	60
T4 – 1.25-in. Horticube® XL (BG)	20	60
T5 - 1-in. Horticube® XL (TG)	20	60
T6 – 1-in. Horticube® XL (BG)	20	60
Total	**120**	**7200**

Type III Tests of Fixed Effects				
Effect	Num DF	Den DF	F Value	Pr > F
treatment	5	114	20.47	<.0001

Analysis

Treatment groupings were analyzed to draw conclusions about the effectiveness of each substrate in satisfying the experimental objectives of increasing germination rate and yield. Binomial germination data were analyzed using statistical analysis software (SAS© 9.4) under logistical regression statistical tests. Germination data were expressed as germination rate (%) and yield as total fresh shoot mass (g). Yield data were analyzed using ANOVA testing procedures. Yield was expressed as total harvest fresh mass (g). Yields were analyzed using Tukey's statistical test at the 95% confidence level. SAS© was coded to use GLIMMIX analysis to account for type two error that occurs in randomized design studies.

Results and Discussion

To determine a final substrate for use in the LED wavelength experiments, germination rates (%) and fresh yields (g) were analyzed to determine which resulted in higher germination rates and fresh yields. The following data show the results of the two germination studies and yield trial testing different germination factors (material, thickness, seeding rate); (Figures 4.4 and 4.5). The third experiment tested yield under the top performing substrates (Table 4.4 and Figure 4.6). Substrate treatment resulted in statistically significant impacts to germination rate ($p < 0.0001$, Table 4.3). The l.5-in. Rootcube® resulted in the highest germination rate (0.80).

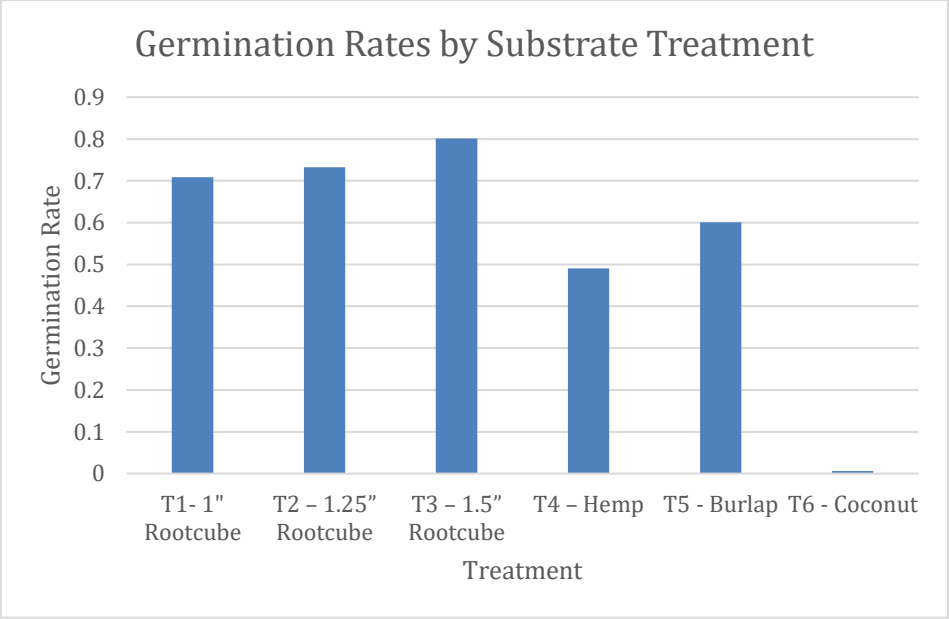


Figure 4.4 Germination rates collected during initial substrate material trial using a seeding rate of 0.05 g/cm².

Coconut resulted in an average germination rate of 0.006 under the tested watering system due to its coarse pore size and low water holding capacity. Artificial media performed better than natural substrates tested. This is partially attributable to the uniform porosity of artificial media tested, where the plant fibers tested contained irregular and large pore sizes which affected the water holding capacity over a 24-hour period. Physical characteristics impacted the ability of the substrate to imbibe and hold water, which affected germination rate (Figure 4.4).

As seed-cell spacing decreased by 33%, germination rate decreased by 11.5%. As seed-cell spacing decreased, germination rate also decreased. The second study examined the effects of substrate configuration on germination success in hydroponic NFT culture. Table 4.3 shows the results of logistical regression for the second germination study which tested substrate configuration.

Substrate treatment had a statistically significant impact on germination rate ($p < 0.0001$, Table 4.3). The 1.5-in. Horticube® substrate resulted in the highest germination rate ($p = 0.63$) compared to the 1.25-in. Horticube ($p = 0.27$). Germination rate approximately doubled in top grooving configurations versus bottom grooving. This mirrors the result in the previous study, where increased distance from the water table decreased germination rates between the 3 mm thick burlap and 10 mm thick coconut substrates. Figure 4.5 shows the results of logistical regression on germination rate for the substrate configuration study.

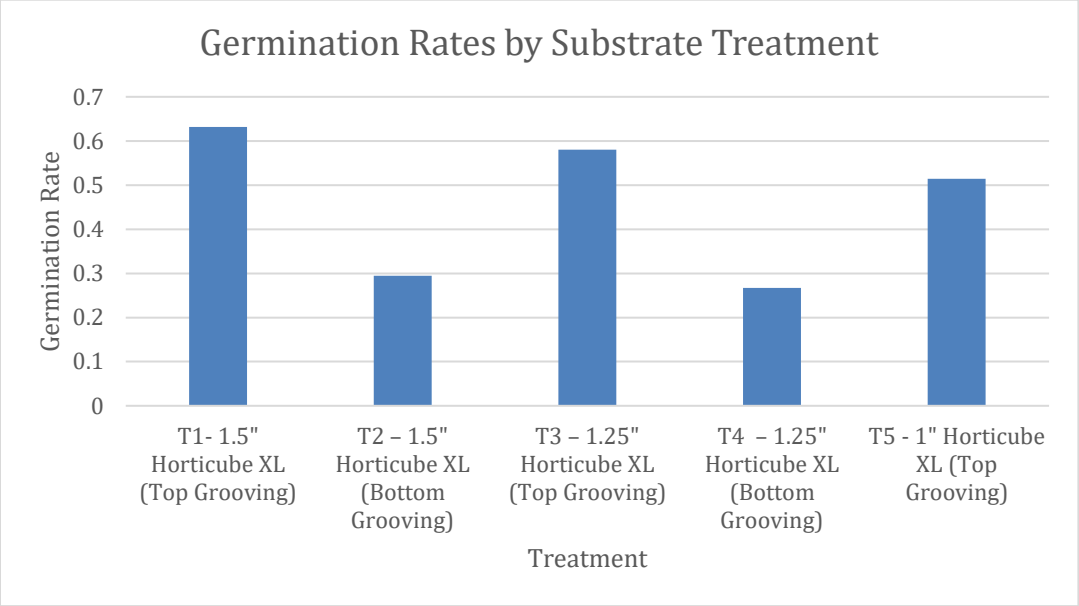


Figure 4.5 Germination rates collected during substrate configuration study using a seeding rate of 0.05 g/cm²

A similar trend as noted before exists between decreasing seed-cell spacing and germination rate. As seed-cell spacing decreased by 33%, the germination rate dropped by 18.6%. The average modeled germination rate for top-grooved substrates was 0.575. For bottom-grooved treatments, the average germination rate was extremely low at 0.281. Bottom grooving configuration exposed seeds to light and elevated them by 1 cm. Studies were performed in consecutive order to allow for analysis of data and selection of new substrates in the following experiments.

Once the effects of substrate material and configuration were more understood, the top performing substrates with relatively high available seeding area were used to conduct a yield trial.

The yield trial determined the effect of substrate treatment on total fresh cilantro yield in the growth chamber. were chosen based on their effectiveness in successfully germinating seeds. Table 4.4 shows the fresh yield data collected 21 days after sowing in the yield trial. During the yield trial, 20 total replicates were exposed to 3500K 90CRI broad-spectrum under five different substrate treatments. All groups received white LED light starting the ninth day after sowing (250 $\mu mol \cdot m^{-2} \cdot s^{-1}$ PAR with a 12-hour photoperiod). Yields were harvested on the 21st day from substrates which resulted in higher germination rates in previous studies. Mean values represent total FM of microgreen plants using 28.5 g seed per treatment replicate (1700 cm^2) Light treatments were applied to four treatment replicates per each of five-1700 cm^2 treatment zones (DF = 4) as sole-source light, totaling 20 sampled replicates.

Table 4.4 Average values for cilantro (*Coriandrium sativum* L. var *'Santo')* microgreen shoot fresh mass (FM) data when grown in controlled environments under different substrate materials with top grooving configuration. The logistical regression results are shown to the right of the experimental data.

Substrate treatment	Replicates per treatment	Average FM (g)
1.5-in. Rootcube®	4	39.42 a
1.25-in. Rootcube®	4	33.54 a
1.5-in. Horticube® XL	4	19.07 b
1.25-in. Horticube® XL	4	9.81 c
1-in. Horticube® XL	4	7.40 c
$LSD_{\alpha=0.05}$		7.52

Type III Tests of Fixed Effects				
Effect	Num DF	Den DF	F Value	Pr > F
Treatment	4	15	32.43	<.0001

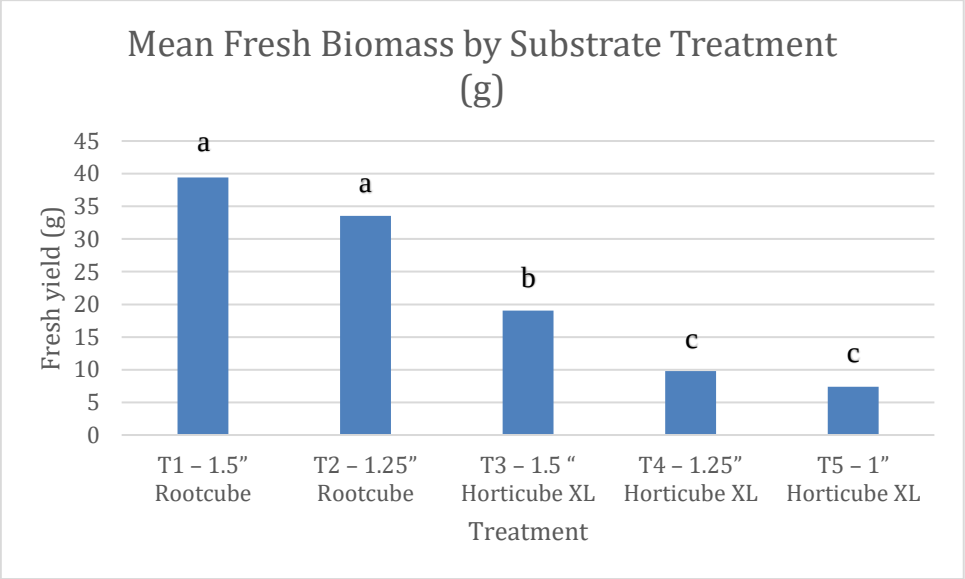


Figure 4.6 Fresh cilantro microgreen biomass yields collected during substrate trial using a seeding rate of 28.5 g/1700 cm².

Substrate treatment had a statistically significant impact on fresh biomass produced by the crop ($p < 0.0001$, Table 4.4). The 1.5-in. Rootcube® produced an average yield of 39.42 grams. Both Rootcube® configurations produced higher yields compared to the Horticube® substrates. Figure 4.6 shows the fresh yields collected 21 days after sowing. Decreasing seed-cell spacing decreased yields. In the Horticubes®, fresh yield decreased by 61.1% with a 33% decrease in seed-cell spacing. In the Rootcubes®, yield decreased by 14.9% alongside a 16% decrease in seed-cell spacing. These results suggest that increasing seed-cell spacing can increase yields at a given seeding rate.

CHAPTER 5: THE EFFECTS OF SELECT NARROW-BAND LIGHT WAVELENGTHS ON CILANTRO YIELD

Introduction

Following the methods of Kopsell and Sams (2013), cilantro (*Coriandrum sativum* L. var. '*Santo*') microgreens were grown in controlled environmental conditions before studying the impacts of narrow-band LED treatments. A broad-spectrum white LED control and five LED light treatments were used. Four of the treatments supplemented broad-spectrum white light with different narrow-band light wavelengths (Ultraviolet: 400 nm, blue: 450 nm, red: 660 nm, and infrared: 740 nm) to stimulate a variety of growth responses from the plants. A fifth light treatment consisted of the four narrow-band wavelengths and lacked a broad-spectrum component. Researchers hypothesized that exposure to only four narrow-band wavelengths from LEDs will increase harvestable dry mass content compared to the broad-spectrum control but may reduce fresh yields. The central hypothesis was that, between the treatments tested, using different narrow-band wavelengths will produce positive and negative effects on harvested fresh and dry mass content.

Materials and Methods

Four LED wavelength studies were conducted between February 4th and May 28th, 2019 using the following substrates: burlap, 1-in. Rootcubes®, and 1.25-in.

Rootcubes®. These three substrates were chosen due to higher germination rates and FM yields in preliminary trials (Figures 4.3, 4.5, and 4.6). Burlap was chosen due to its relatively low cost and success in earlier trials. Two studies were conducted on burlap and one was performed on both the 1-in. and 1.25-in. Rootcube® substrate. Temperature was held at 16-20°C and relative humidity was maintained between 44-51% by the ventilation system due to the impact these factors have on plant growth and development. Following the methods of Samuolienė et al. (2017), total light intensity remained constant at 250 $\mu mol \cdot m^{-2} \cdot s^{-1}$ PAR between treatment zones.

Kopsell and Sams (2013) discussed that fertility had a direct impact on glucosinolate content in *Brassicaceae* microgreens. No fertility or nutrients was added to the irrigation water to prevent any interaction effect with the light treatments. Seeds were sown directly onto presoaked substrate pieces. Shelves were sub-irrigated with 850-890-mL of non-fertilized municipal water once per day. Light cycles lasted for twelve hours followed by a twelve-hour dark cycle. Six shelves were lined with media and seeded at a seeding rate of 28.5 g seed per 1700 cm^2 sample area. The third LED experiment used a seeding rate of 40 g seed per 1700 cm^2. Trays were placed under light treatments from the ninth day until harvest on the 21st day.

Treatments

Cilantro was grown in the six treatment zones on one substrate at a time. The only treatment factor was the spectral composition of light applied to the plant. The light

wavelength experiment was conducted using different substrates to determine if substrate had an impact on yield under the LED treatments (Table 5.1). Results of isolated light wavelength treatments were quantified by harvesting samples taken from directly beneath the light. The sample zone consisted of a 10 cm width, to ensure light intensity uniformity across the sampled microgreens. This reduced the variability of light intensity in the sampled zone to reduce the likelihood of experimental errors. Four 1700 cm^2 treatment replicates were harvested on the 21st day from each of the six treatment zones, totaling 24 samples per experimental replication.

Table 5.1 Treatment layout of final experiments describing position of treatment zones within the cabinet, quantitative color compositions of the treatments, and light wavelength ranges.

Shelf	Treatment	Nominal color	Light wavelength ranges
1	Broad spectrum control	W	410 – 780 nm
2	Narrow-band infrared	99W1IR	410 – 780 nm; 740±10 nm
3	Narrow-band red	40W60R	410 – 780 nm; 680±10 nm
4	Narrow-band blue	60W40B	410 – 780 nm; 450±10 nm
5	Narrow-band ultraviolet	99W1UV	410 – 780 nm; 400±10 nm
6	Narrow-band isolate spectrum	1IR 59R 39B 1UV	400±10 + 450±10 + 680±10 + 740±10 nm

The control group consisted of warm, broad-spectrum white LED light (Table 5.1). Five treatment groups were treated with sole-source LED light arrays on a twelve-hour light/dark cycle after cotyledon (first leaf) emergence. Four of the five light treatments utilized broad-spectrum white LEDS with supplemental LED light in an isolated wavelength region.

Following the methods of Hammock (2018), a red-blue ratio of 60:40 was used in the narrow band spectrum. The four narrow-band wavelengths were used without a broad spectrum to measure the impact of a narrow-band spectrum on plant growth and dry mass content. A fifth LED treatment, absent of white light, utilized only the four different supplemental light wavelengths, creating a narrow-band spectrum which utilized four light wavelengths shown by studies to impact plant growth and physiology (Figure 5.1).

Two white lights were placed above shelves 1-5, with a total of 10 white LED light bars used. One far-red light (740 nm) was placed over shelves 2 and 6. Two red lights (660 nm) were placed over shelves 3 and 6. Two blue lights (450 nm) were placed above shelves 4 and 6. Two ultraviolet lights (400 nm) were placed above shelves 5 and 6.

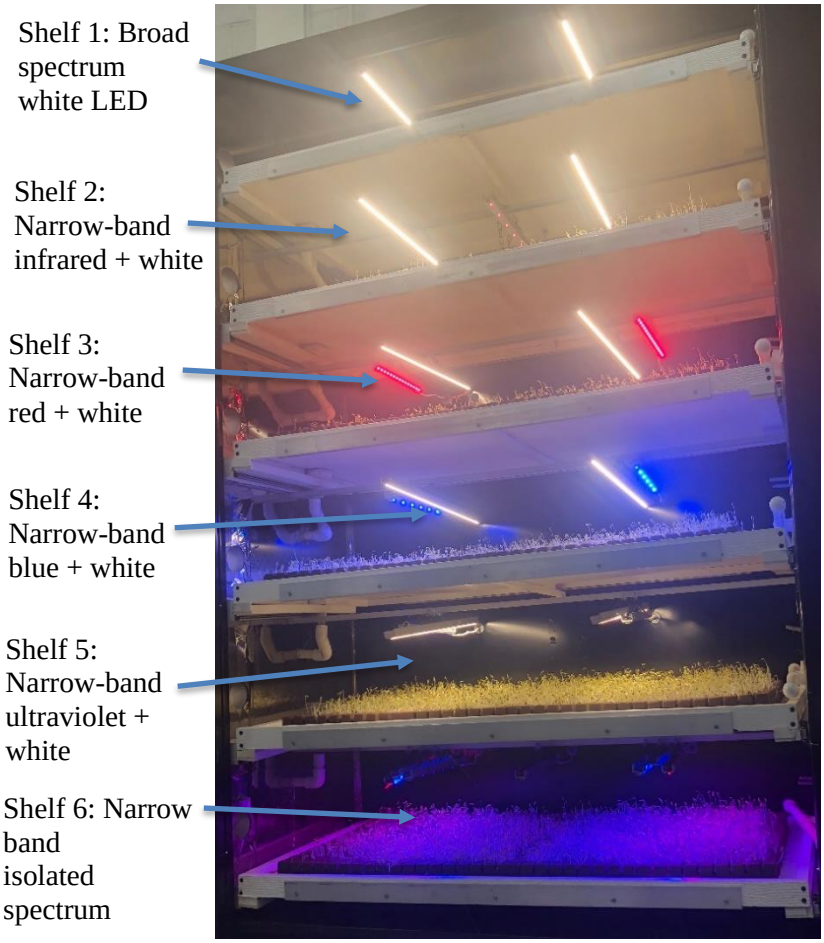


Figure 5.1 Front view of light treatments, showing six treatment shelves. Each of the six 6800 cm² treatment zones contained four 1700 cm² treatment replicates.

Statistical Design

Four 1700 cm² substrate pieces were placed across each treatment zone during each separate cilantro crop cycle. This produced four replicated samples per treatment group in each experiment. A total of 24 samples comprised one experiment's yield data set. Each of the six 6800 cm² treatment zones contained four 1700 cm² treatment replicates, which were separately harvested and analyzed.

Data Collection

Recorded fresh yields were collected by cutting all plant material above the substrate level. Shoots were harvested and analyzed for fresh mass and dry mass percentage from groups receiving individual LED light treatments. Oven-dried and freeze-dried tissue was weighed and divided by original sample mass to calculate dry mass percentage. Twenty grams of fresh tissue from each treatment replicate was oven-dried at 38°C for two days before final dried masses were recorded. Twenty grams of fresh tissue was collected from under the LED lights at four sampling locations per treatment and was immediately stored at -20° C for freeze-drying. The twenty-gram sample was freeze-dried at -60° C and 200 mbar for three days and stored again at -20° C. Both oven and freeze-drying methods were used to determine if both methods provide the same result.

Analysis

Yield was expressed as total harvested fresh mass (g). Dry masses from oven- and freeze-drying from each treatment replicate were used to calculate the percentage on a fresh mass basis. Dry mass percentage was expressed as a percentage of dry mass to original sample mass using both oven- and freeze-drying methods (10 g oven-dried; 20 g freeze-dried). Yield-energy ratio was calculated by multiplying power and total duration of crop cycle (252 hrs.). Fresh biomass yield was divided by energy usage to create a useful metric for growers to use when selecting lighting assemblies based on fresh yield productivity or energy usage.

Results and Discussion

A series of light wavelength experiments were conducted on cilantro in a growth chamber. The following experiments examined the effect of varying light wavelength applications on total fresh yield and dry mass percentage in cilantro microgreens.

The growth chamber was used to produce one crop at a time, under a single substrate type. Twenty grams of fresh tissue from each sample was oven-dried at 38°C for two days. Twenty grams of fresh tissue from each sample was freeze-dried at -60° C and 200 mbar for three days and stored at -20° C.

Spectral Measurements of LED Treatments

LED light spectra for each treatment was measured to give some practical representation of the different treatments which growers can use to calibrate LED spectra. Measurements were taken under the light assemblies using a Lighting Passport Spectrometer (Assensetek© , USA).

This research utilized wavelengths of red (660 nm) and blue (450 nm) light due to their recently discovered effects on photosynthesis and carotenoid pathways. Red light was tested due to its relatively high absorption levels in the chloroplast. Blue light was selected at this wavelength due to its demonstrated effects on carotenoid and nutrient content. Ultraviolet light was used to mimic a natural environmental stress, where plants exposed to sunlight receive some level of ultraviolet light. Infrared light was selected for its ability to maintain healthy stem and leaf development in microgreens.

In Figure 5.2, the photosynthetic photon flux density by wavelength and spectral composition is shown for the Broad-spectrum white LED configuration used in the control group.

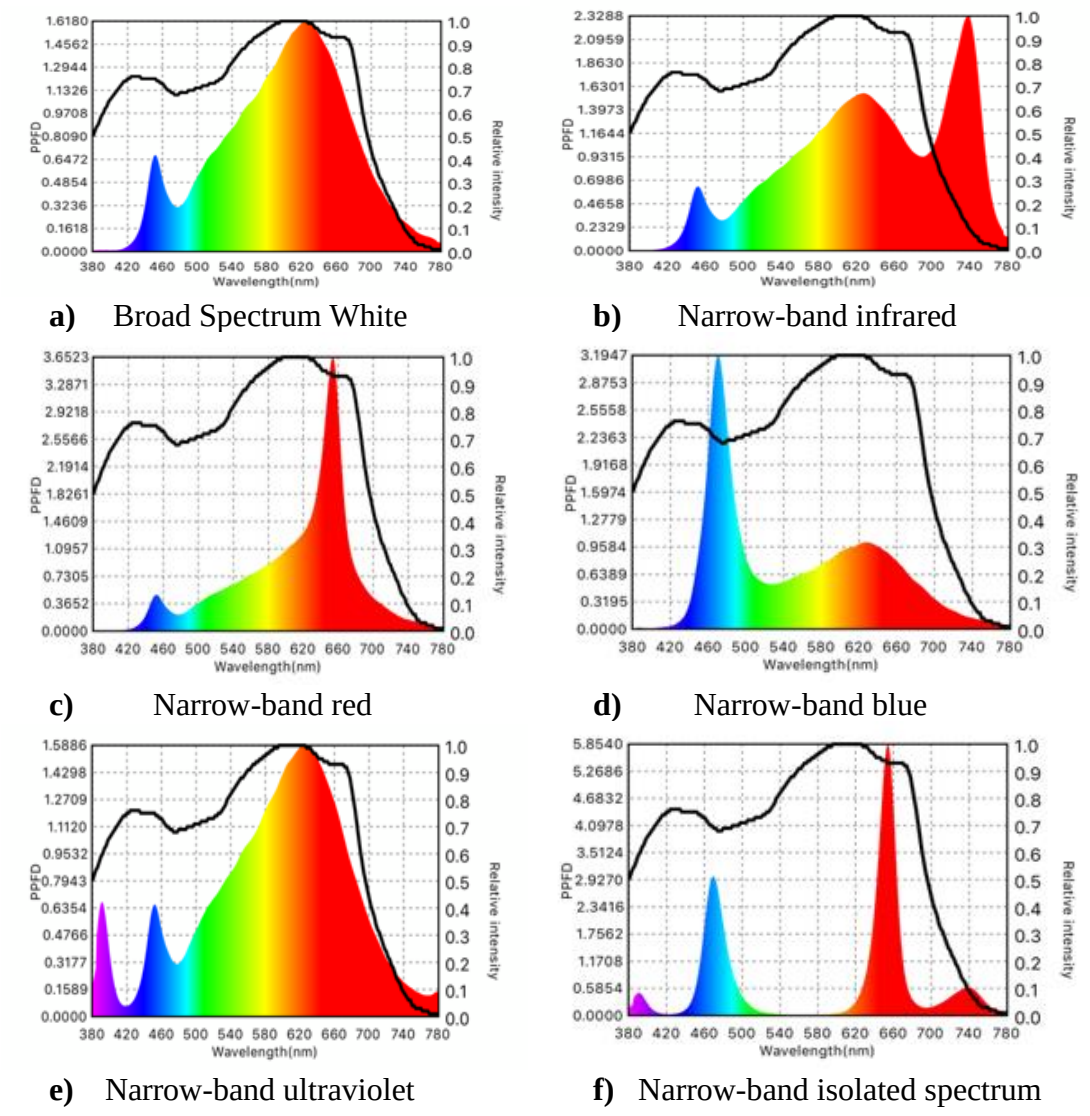


Figure 5.2 Spectral composition and photosynthetic photon flux density (PPFD in $\mu mol \cdot m^{-2} \cdot s^{-1}$ PAR) by wavelength for narrow-band LED treatments. Relative intensity is shown respective to the most intense wavelength.

For example, in Figure 5.2-a, the relative intensity of light at 450 nm is approximately 43% of light intensity at 640 nm. Following Runkle (2016), the peak infrared wavelength (b) was selected at 740 nm due to its ability to impact plant photoreceptor activity and increase the far-red: red ratio. McCree's (1971) work found that light in the 650-700 nm region is mostly absorbed by chlorophyll in conducting photosynthesis. The peak wavelength (c) was selected at 660 nm to promote a high rate of photosynthesis based on its accepted quantum absorption levels in plant leaf tissue. Following the methods of Kopsell et al. (2017), the narrow-band blue supplementation group had its peak wavelength (d) selected at 450 nm to promote increased metabolite content. In accordance with Stapleton (1992), the supplemental ultraviolet wavelength (e) was chosen at 400 nm due to its ability to signal environmental stress in plants. Spectral characteristics are shown for the narrow-band isolated spectrum (f). The four studies performed used different substrates and an increased seeding rate to determine impact on yield (Table 5.2).

Table 5.2 Overview of LED experiments, describing sequence, substrate type, and seeding rate.

LED Experiment	Substrate	Seeding rate
1	1.25-in. Rootcube®	28.5 g seed/ 1700 cm^2
2	1-in. Rootcube®	28.5 g seed/ 1700 cm^2
3	Burlap	40 g seed/ 1700 cm^2
4	Burlap	28.5 g seed/ 1700 cm^2

Four crops were grown under LED treatments using the following sequence of substrates: 1.25-in. Rootcube®, 1-in. Rootcube®, and burlap twice. A burlap trial was performed at a higher seeding rate (40 g seed per 1700 cm²) to determine if yields could be further increased. The other three studies used a seeding rate of 28.5 g seed per 1700 cm². All four studies used a light intensity 250 μmol·m^{-2}·s^{-1} PAR with a 12-hour photoperiod. The 1.25-in. Rootcube® was first used to grow cilantro under the LED treatments due to the high yields (33.4 g) that resulted in the previous study along with its higher seeding area than the 1.5-in. configuration. All six treatments (DF = 5) were exposed to 250 μmol·m^{-2}·s^{-1} PAR with a 12-hour photoperiod.

Yields were harvested on the 21st day and underwent FM and %DM analysis. Mean values represent total FM of microgreen plants using 28.5 g seed per treatment replicate (1700 cm²). Light treatments were applied to four sampled treatment replicates across six-1700 cm² treatment zones (n = 24; 4 per treatment) as sole-source light. (Table 5.3).

Red light supplementation resulted in the lowest dry mass percentage recorded (8.7%). Higher proportions of red light increased yields but decreased total dry mass content. Narrow-band red (660 nm) light lowered the dry mass percentage while increasing fresh yields. Narrow-band blue (450 nm) light raised dry mass percentage while lowering fresh yields.

Table 5.3 Average values for cilantro (*Coriandrium sativum* L. var *'Santo')* microgreen shoot fresh mass (FM) and dry mass percentage (%DM) when grown in a controlled environment using 1.25-in. seed cell spacing. Yield-energy ratio is shown for each treatment over the entire crop cycle, calculated using electrical power consumption (W) * cycle length (252 hrs.).

Light Treatment	Light wavelength ranges	FM (g)	%DM (Oven-Dried)	Yield-energy ratio (g/kW·h)
W	410 – 780 nm	42.45 b	11.1% a	6.06
99W1IR	410 – 780 nm; 740±10 nm	43.09 b	11.2% a	6.84
40W60R	410 – 780 nm; 680±10 nm	55.18 a	8.7% a	8.80
60W40B	410 – 780 nm; 450±10 nm	40.16 b	12.8% a	6.56
99W1UV	410 – 780 nm; 400±10 nm	43.65 b	11.2% a	6.21
1IR 59R 39B 1UV	400±10 + 450±10 + 680±10 + 740±10 nm	39.56 b	12.3% a	5.18
$LSD_{\alpha=0.05}$		7.45	2.6%	

Light treatment had a statistically significant impact on fresh biomass produced by the crop ($p = 0.004$, Table 5.3). Light treatment was not statistically significant on dry mass percentage ($p = 0.068$) using the oven-drying method. The white light was supplemented with red light (660 nm). The result was a biomass increase by 30% over the control that used 10.3% less electrical power. Narrow-band red light supplementation was 45% more effective at producing yields per unit energy than the control. Figures 5.3 and 5.4 display the average fresh yield and dry mass percentages from the study. Red light (660 nm) supplementation increased yields relative to the control. The narrow-band spectrum lowered fresh yields, but without a statistically significant difference.

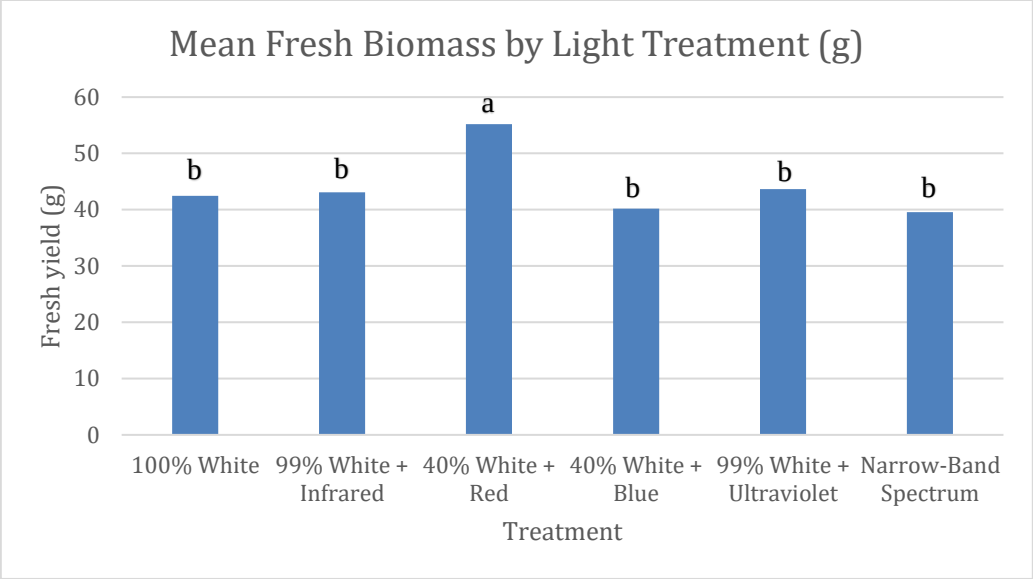


Figure 5.3 Fresh cilantro microgreen biomass yields collected using 1.25-in. Rootcube® substrate.

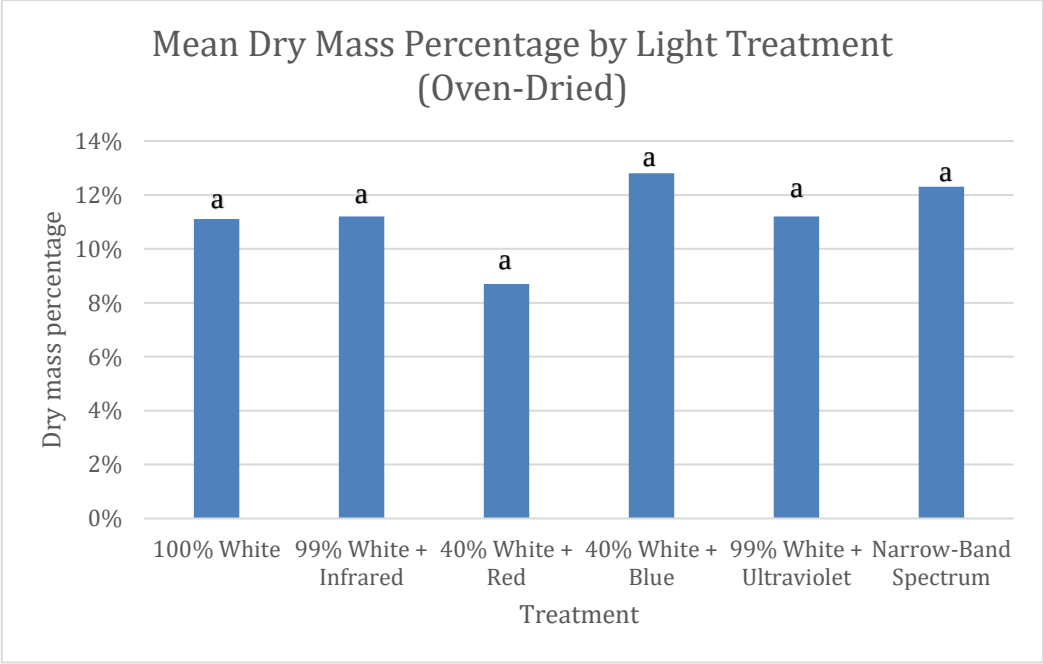


Figure 5.4 Oven-dried mass percentages collected during the 1.25-in. Rootcube® trial using a seeding rate of 28.5 g/1700 cm².

These results suggest that supplementing white light with narrow-band red light (660 nm) can increase fresh microgreen biomass. Narrow-band blue light (450 nm) increased dry mass percentage relative to the control but with no statistical significance. Red light (660 nm) supplementation resulted in the lowest dry mass percentage of all treatments tested with no statistical significance.

All six treatments (DF = 5) were exposed to 250 $\mu mol \cdot m^{-2} \cdot s^{-1}$ PAR with a 12-hour photoperiod. Yields were harvested on the 21st day and underwent FM and %DM analysis. Mean values represent total FM of microgreen plants using 28.5 g seed per treatment replicate (1700 cm^2). Light treatments were applied to four sampled treatment replicates across six-1700 cm^2 treatment zones (n = 24; 4 per treatment) as sole-source light.

The 1-in. Rootcube® material was used in the next study. Table 5.4 shows the average fresh yield and dry mass percentages from the second study. Light treatment did not have a statistically significant impact on fresh biomass collected from the crop ($p = 0.16$, Table 5.4). The 1-in. Rootcube® material was used in this study. Figure 5.5 displays the average fresh yield from the second study.

Table 5.4 Average values for cilantro (*Coriandrium sativum* L. var *'Santo')* microgreen shoot fresh mass (FM) and dry mass percentage (%DM) when grown in a controlled growth chamber using 1-in. seed cell spacing. Yield-energy ratio is shown for each treatment over the entire crop cycle, calculated using power consumption (W) and production cycle length (252 hrs.).

Light Treatment	Light wavelength ranges	FM (g)	%DM (Oven-Dried)	%DM (Freeze-Dried)	Yield-energy ratio (g/kW·h)
W	410 – 780 nm	49.34 a	11.0% a	12.1% ab	7.05
99W1IR	410 – 780 nm; 740±10 nm	51.42 a	10.3% a	11.2% bc	8.16
40W60R	410 – 780 nm; 680±10 nm	57.00 a	7.9% a	9.8% c	9.09
60W40B	410 – 780 nm; 450±10 nm	53.29 a	8.7% a	11.8% ab	8.71
99W1UV	410 – 780 nm; 400±10 nm	43.84 a	9.4% a	12.0% ab	6.24
1IR 59R 39B 1UV	400±10 + 450±10 + 680±10 + 740±10 nm	47.62 a	9.0% a	13.1% a	6.23
$LSD_{\alpha=0.05}$		10.13	2.2%	1.8%	

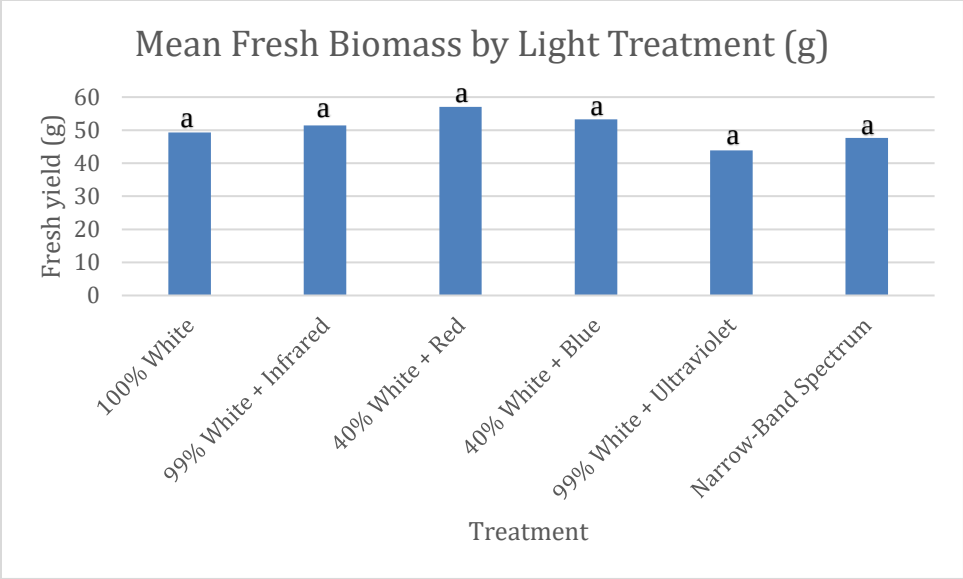


Figure 5.5 Fresh cilantro microgreen biomass yields collected using 1-in. Rootcube® substrate.

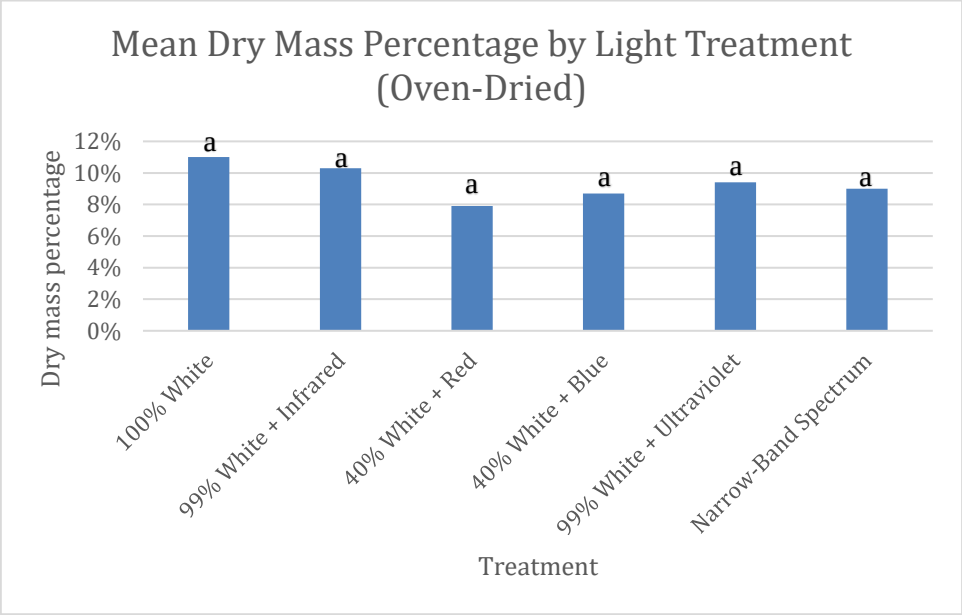


Figure 5.6 Oven-dried mass percentages collected during the 1-in. Rootcube® trial using a seeding rate of 28.5 g/1700 cm².

Supplementing white light with red light (660 nm) slightly increased total fresh yield while also decreasing dry mass. Red light supplementation increased yield per unit energy by 29% relative to the broad-spectrum control. This is a similar result to the previous study, where fresh mass per unit energy increased 1.45 times that of the control. Figure 5.6 displays the average oven-dried mass percentages from the second study. Again, oven-drying did not result in significant impacts on dry mass percentage ($p = 0.08$). In this study, red light supplementation resulted again in the lowest dry mass percentage (7.9%) through oven-drying. These results suggest that light treatment may not have a significant impact in dry mass content that is detectable by oven-drying. Figure 5.7 displays the average freeze-dried mass percentages from the second study.

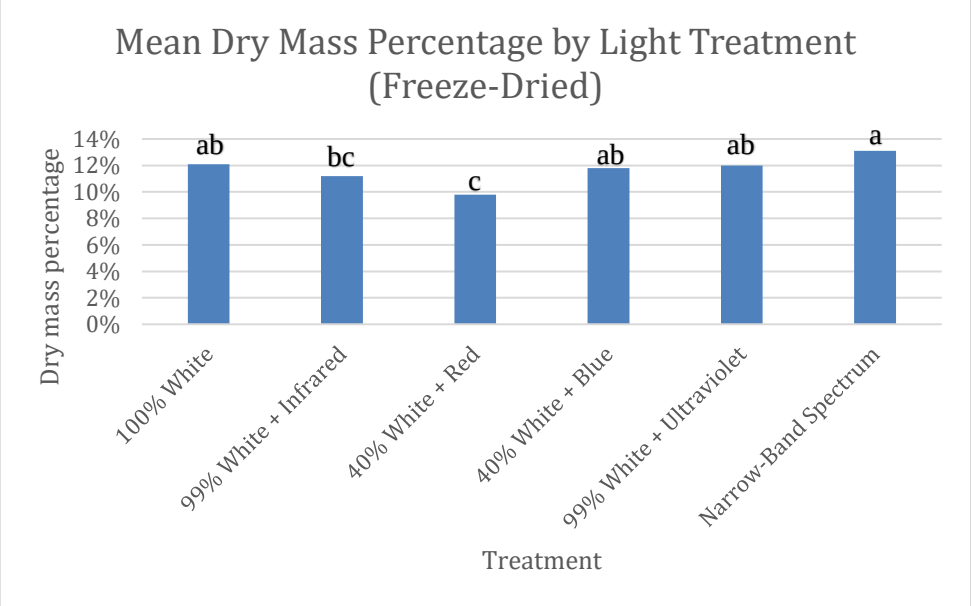


Figure 5.7 Freeze-dried mass percentages collected during the 1-in. Rootcube® trial using a seeding rate of 28.5 g/1700 cm².

However, when using the freeze-drying method, statistically significant differences were detected between the treatment groups ($p = 0.03$). The narrow-band spectra resulted in 34% higher dry mass than narrow band red treatments (13.1%) without a significant reduction in yield. Red light supplementation resulted in the lowest dry mass percentage (9.8%). These results suggest that narrow-band spectra increase the total dry mass percentage while maintaining fresh yields. Narrow-band spectrum was the most effective method tested at increasing crop dry mass percentage.

All six treatments (DF = 5) were exposed to 250 $\mu mol \cdot m^{-2} \cdot s^{-1}$ PAR with a 12-hour photoperiod. Yields were harvested on the 21st day and underwent FM analysis. Mean values represent total FM of microgreen plants using 40.0 g seed per treatment replicate (1700 cm^2). Light treatments were applied to four sampled treatment replicates across six-1700 cm^2 treatment zones (n = 24; 4 per treatment) as sole-source light. Table 5.5 displays average fresh yield from the third light spectrum study. Burlap substrate was used in this study following the two previous studies that used artificial media due to its performance in earlier trials and low cost.

Increased red light levels produced the highest fresh yield overall but without statistical significance. Yield increased as seeding rate was increased from 28.5 to 40 g/ 1700 cm^2.

Table 5.5 Average values for cilantro (*Coriandrium sativum* L. var *'Santo')* microgreen shoot fresh mass (FM) when grown in a controlled growth chamber using burlap. Yield-energy ratio is shown for each treatment over the entire crop cycle, calculated using power consumption (W) and production cycle length (252 hrs.).

Light Treatment	**Light wavelength ranges**	**FM (g)**	**Power per treatment (W)**	**Yield-energy ratio (g/kW·h)**
W	410 – 780 nm	77.85 a	27.8	11.12
99W1IR	410 – 780 nm; 740±10 nm	64.14 a	25.0	10.18
40W60R	410 – 780 nm; 680±10 nm	79.81 a	24.9	12.73
60W40B	410 – 780 nm; 450±10 nm	55.23 a	24.3	9.02
99W1UV	410 – 780 nm; 400±10 nm	78.59 a	27.9	11.18
1IR 59R 39B 1UV	400±10 + 450±10 + 680±10 + 740±10 nm	29.57 b	30.3	3.87
$LSD_{\alpha=0.05}$		24.96		

Light treatment had a statistically significant impact on fresh biomass collected from a single treatment group ($p = 0.003$, Table 5.5). There was a statistically significant decrease in yield in the narrow-band spectrum group not reflected in the previous experiments (Figure 5.8). All six treatments (DF = 5) were exposed to 250 $\mu mol \cdot m^{-2} \cdot s^{-1}$ PAR with a 12-hour photoperiod. Mean values represent total FM of microgreen plants using 40.0 g seed per treatment replicate (1700 cm^2). Light treatments were applied to four sampled treatment replicates across six-1700 cm^2 treatment zones (n = 24; 4 per treatment) as sole-source light. Burlap substrate was used in this study due to its adequate performance in initial trials and low cost. The sharp yield reduction in the narrow-band group compared to the control is not reflected in any other experimental result.

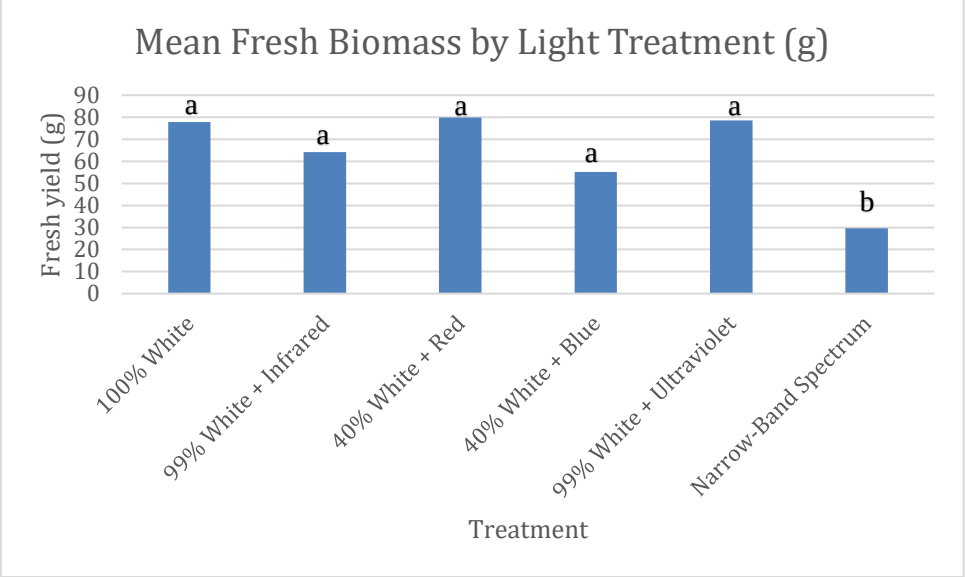


Figure 5.8 Fresh cilantro microgreen biomass yields collected using burlap as a substrate.

This yield reduction is attributed to visually noticeable fungal pressure caused by increased seeding rate and lack of broad-spectrum light. Fungal pressure may have been due to the high carbon-content of the natural burlap fiber resulting in increased microbial growth rates.

Table 5.6 and Figures 5.9 and 5.10 display the average fresh yield and dry mass percentages from the fourth and final study. Yields were harvested on the 21st day and underwent FM and %DM analysis.

Table 5.6 Average values for cilantro (*Coriandrium sativum* L. var *'Santo')* microgreen shoot fresh mass (FM) and dry mass percentage (%DM) when grown in a controlled growth chamber using burlap. Yield-energy ratio is shown for each treatment over the entire crop cycle, calculated using power consumption (W) * cycle length (252 hrs.).

Light Treatment	Light wavelength ranges	FM (g)	%DM (Freeze-Dried)	Power per treatment (W)	Yield-energy ratio (g/kW·h)
W	410 – 780 nm	41.91 a	12.7% a	27.8	5.99
99W1IR	410 – 780 nm; 740±10 nm	46.79 a	10.7% b	25.0	7.43
40W60R	410 – 780 nm; 680±10 nm	38.13 a	11.0% b	24.9	6.08
60W40B	410 – 780 nm; 450±10 nm	43.57 a	9.8% b	24.3	7.12
99W1UV	410 – 780 nm; 400±10 nm	41.30 a	10.0% b	27.9	5.87
1IR 59R 39B 1UV	400±10 + 450±10 + 680±10 + 740±10 nm	44.92 a	9.8% b	30.3	5.88
$LSD_{\alpha=0.05}$		9.014	1.5%		

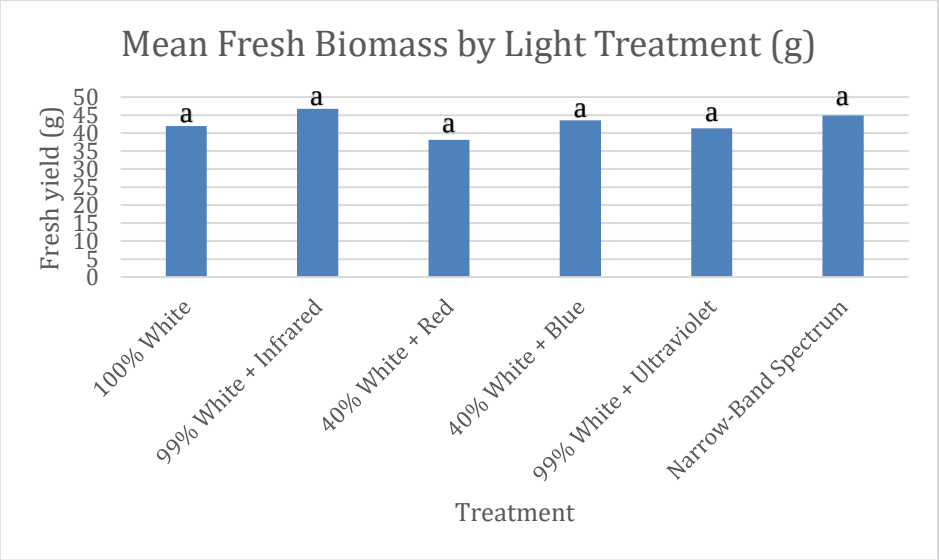


Figure 5.9 Fresh cilantro microgreen biomass yields collected during the burlap trial using a seeding rate of 28.5 g/1700 cm².

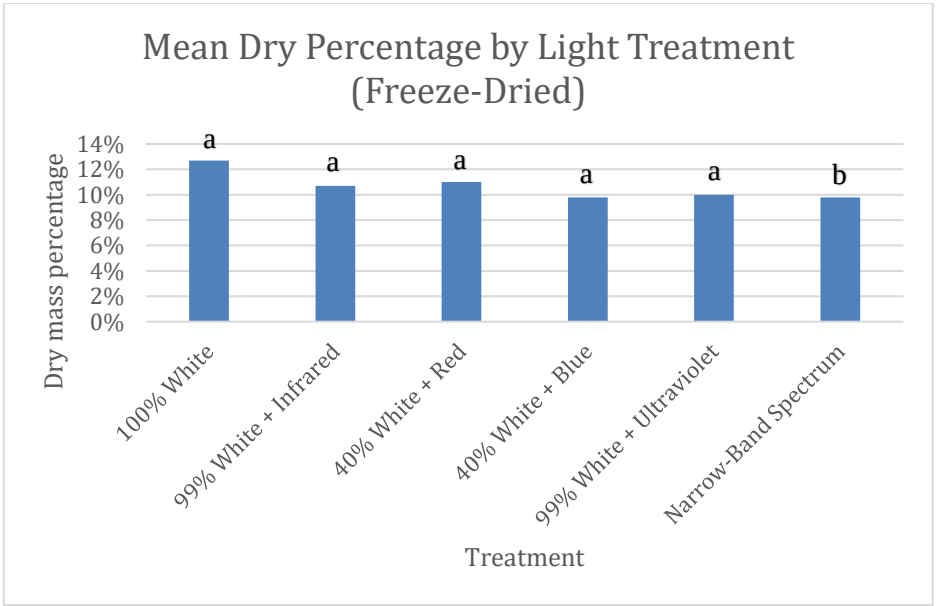


Figure 5.10 Freeze-dried mass percentages collected during the burlap trial using a seeding rate of 28.5 g/1700 cm².

Light treatment had no statistically significant impact on fresh yield collected ($p = 0.44$, Table 5.6). Again, freeze-drying showed a statistically significant impact on dry mass percentage in the control group ($p = 0.006$). The control group resulted in the highest dry mass percentage (12.7%) from freeze-drying. This does not reflect the results in the 1.25-in. Rootcube© trial (Table 5.3). This can be attributed to known variation in temperature and humidity between experiments, but that is only suggested by the data. Visual representation of the harvested fresh biomass can be found in Figure 5.9.

Interestingly, infrared (740 nm) supplementation resulted in the highest fresh yields. This was not reflected in any other result. It may have been caused by an accelerated evaporation from the plant leaf surface caused by high proportions of radiation in the infrared zone (700 nm-1 mm) which easily heat up surrounding surfaces. These results suggest that light treatment had no impact on fresh biomass produced, but environmental factors potentially impacted growth rates in the treatment areas. The freeze-dried mass percentages are shown in Figure 5.10. The broad-spectrum white control resulted in the highest dry mass content in the final experiment. This could have been due to the burlap substrate that was used, due to it having a different porosity and water holding capacity than the other tested substrates. Fertility could also have played a role in this phenomenon, as the Rootcubes© tested contain an undisclosed quantity of dolomitic lime.

CHAPTER 6: CONCLUSIONS AND RECOMMENDATIONS

Cilantro var. *'Santo'* can be effectively grown indoors in the total absence of natural light using LEDs. The choice of substrate impacted crop production both in germination and vegetative phases. Rootcubes® performed better than any other substrate tested at germination and produced the highest yields. As substrate thickness increased, germination rate decreased. Substrate plays a critical role in microgreen production by staging water, air, and nutrients at optimal levels for the plant.

Supplementation of individual light wavelengths may provide an effective tool for increasing profitability in commercial production. Narrow-band supplementation of white light using red (660 nm) light can be used to increase yield productivity and reduce energy costs for growers. Red light should be supplemented in situations where fresh mass is prioritized for energy savings. In dried herb operations for vitamin or spice production, red light supplementation can still be used effectively, as it decreased dry mass percentage by 22% but is offset by the 30% yield increase. Oven-drying and freeze-drying produced different results from the same sampling groups suggesting that freeze-drying is a more reliable method of preserving sample quality.

The reduced impacts of blue and narrowband treatments in burlap trials may be caused by a lack of nutrient content within the burlap substrate. This does not reflect the results obtained in studies using Rootcube® media, which contain dolomitic lime. The data suggest that the impact of light treatment on dry mass may be related to

substrate fertility. Burlap substrate provided less protection to the roots from ambient oxygen in the surrounding atmosphere, which may oxidize root tissues, impacting crop metabolism. Burlap is a high-performing substrate relative to its cost in terms of fresh yield, but Rootcube® media should be used if successful germination is more important than yield, as in settings where substrates are being used to propagate seed for transplant into a hydroponic system. Shorter seed-cell spacing may provide more available seeding area, but counterintuitively results in reduced germination and yield.

At increased seeding rates (40 g per 1700 cm^2), the narrow-band spectrum reduced fresh yields by 29% relative to the broad-spectrum white control. The reduction was likely due to mold development on the substrate material. The fungal onset could have resulted from increased moisture retention in more densely seeded areas. The higher seeding rate combined with a narrow-band spectrum resulted in the onset of fungus by the 14^{th} day, which provided a diminished yield and high risk of crop failure. This narrow-band light treatment is absent of most of the light wavelengths contained in other light treatments. Absence of broad-spectrum light may have promoted mold growth, which did not noticeably impact the other treatments in this experiment. Yield and seeding rate were positively correlated in other treatment groups, where broad-spectrum light was present to limit fungal growth. Increased seeding rate resulted in a thicker canopy, which promoted fungal growth by retaining more moisture and by blocking light and air from entering the foliar canopy. Last, fan capacity should be increased above 2.83 m^3/min to limit fungal development.

REFERENCES

Ahmed, N., Choe, Y., Mustad, V. A., Chakraborty, S., Goates, S., Luo, M., & Mechanick, J. I. (2018). Impact of malnutrition on survival and healthcare utilization in Medicare beneficiaries with diabetes: a retrospective cohort analysis. *BMJ Open Diabetes Research & Care*, *6*(1). doi: 10.1136/bmjdrc-2017-000471

Al-Kodmany, K. (2018). The Vertical Farm: A Review of Developments and Implications for the Vertical City. *Buildings*, *8*(2), 24. doi: 10.3390/buildings8020024

Behdarvandi, Behrang, "Comparative study of factors influencing seed germination and seedling longevity in Cuscuta (dodder, Convolvulaceae)" (2014). Theses and Dissertations (Comprehensive). 1689. http://scholars.wlu.ca/etd/1689

Bewley, D. J., Black, M. (1985) Seeds: physiology of development and germination. New York: Plenum.

Biswas, M. (1986). International Cooperation in Nutrition. In *the Thirteenth International Congress of Nutrition* (pp. 87-88). Food Policy.

Bouis, H. E., & Saltzman, A. (2017). Improving nutrition through biofortification: A review of evidence from HarvestPlus, 2003 through 2016. *Global food security, 12*, 49–58. doi:10.1016/j.gfs.2017.01.009

Brazaitytė, A., Sakalauskienė, S., Samuolienė, G., Jankauskienė, J., Viršilė, A., Novičkovas, A., Duchovskis, P. (2015). The effects of LED illumination spectra and intensity on carotenoid content in Brassicaceae microgreens. *Food Chemistry, 173*, 600-606. doi:10.1016/j.foodchem.2014.10.077

Cawley J. and Meyerhoefer C. (2012). The Medical Care Costs of Obesity: An Instrumental Variables Approach. *Journal of Health Economics*, 31(1): 219-230.

Cediel, G., Olivares, M., Brito, A., Cori, H., & Romaña, D. L. D. (2015). Zinc Deficiency in Latin America and the Caribbean. *Food and Nutrition Bulletin*, *36*(2_suppl): 129-138. doi: 10.1177/0379572115585781

Chenard, C. A., Zimmerman, M. B., Smith, K. L., Nonnie, P. F., & Wahls, T. L. (2015). New Measured Weight for One Cup Raw Kale Reduces Nutrient Intake of Individuals Following the Wahls™ Diet. *Procedia Food Science*, *4*, 39–47. doi: 10.1016/j.profoo.2015.06.007

Cooper, A. J. (1996). *The ABC of NFT: Nutrient film technique: The world's first method of crop production without a solid rooting medium*. Narrabeen, N.S.W.: Casper Publications.

Covell, S., Ellis, R. H., Roberts, E. H., & Summerfield, R. J. (1986). The Influence of Temperature on Seed Germination Rate in Grain Legumes. *Journal of Experimental Botany*, *37*(5), 705–715. doi: 10.1093/jxb/37.5.705

Cummings, I. G., Reid, J. B., & Koutoulis, A. (2007). Red to far-red ratio correction in plant growth chambers? growth responses and influence of thermal load on garden pea. *Physiologia Plantarum,131*(2): 171-179. doi:10.1111/j.1399-3054.2007.00958.x

Darko, E., Heydarizadeh, P., Schoefs, B., & Sabzalian, M. R. (2014). Photosynthesis under artificial light: The shift in primary and secondary metabolism. *Philosophical Transactions of the Royal Society B: Biological Sciences,369*(1640), 20130243. doi:10.1098/rstb.2013.0243

DeFries, R., and F. Achard (2002), New estimates of tropical deforestation and terrestrial carbon fluxes: Results of two complementary studies, LUCC Newsl., 8, 7 – 9.

Despommier, D. (2013). Farming up the city: the rise of urban vertical farms. *Trends in Biotechnology*, *31*(7), 388–389. doi: 10.1016/j.tibtech.2013.03.008

Diouf, M., Samba, S. A. N., Ndoye, O., & Damme, P. V. (2015). Difference in germination rate of Baobab (Adansonia digitata L.) provenances contrasting in their seed morphometrics when pretreated with concentrated sulfuric acid. *African Journal of Agricultural Research*, *10*(12), 1412–1420. doi: 10.5897/ajar2014.9426

Doll, R., & Peto, R. (1981). The Causes of Cancer: Quantitative Estimates of Avoidable Risks of Cancer in the United States Today. *JNCI: Journal of the National Cancer Institute*, *66*(6), 1192–1308. doi: 10.1093/jnci/66.6.1192

Foley, J. A. (2005). Global Consequences of Land Use. *Science*, *309*(5734), 570–574. doi: 10.1126/science.1111772

Hammock, Hunter Albright, "The Impact of Blue and Red LED Lighting on Biomass Accumulation, Flavor Volatile Production, and Nutrient Uptake in Hydroponically Grown Genovese Basil. " Master's Thesis, University of Tennessee, 2018. https://trace.tennessee.edu/utk_gradthes/5083

Hemming, S. (2011). Use of Natural and Artificial Light in Horticulture - Interaction Of Plant And Technology. *Acta Horticulturae*, (907), 25–35. doi: 10.17660/actahortic.2011.907.1

Houghton, R. A. (2003). Why are estimates of the terrestrial carbon balance so different? *Global Change Biology*, *9*(4), 500–509. doi: 10.1046/j.1365-2486.2003.00620.x

Huang, S., Frizzi, A., Florida, C. A., Kruger, D. E., & Luethy, M. H. (2006). High Lysine and High Tryptophan Transgenic Maize Resulting from the Reduction of Both 19- and 22-kD α-zeins. *Plant Molecular Biology*, *61*(3), 525–535. doi: 10.1007/s11103-006-0027-6

International Seed Testing Association. (2020). International Rules for Seed Testing, Chapter 7, i–7-6 (14) https://doi.org/10.15258/istarules.2020.07

Kaiser, C. and M. Ernst. (2018). *Microgreens.* Center for Crop Diversification, University of Kentucky College of Agriculture, Food and Environment. Retrieved from http://www.uky.edu/ccd/sites/www.uky.edu.ccd/files/microgreens.pdf

Khoo, C. S., & Knorr, D. (2014). Grand Challenges in Nutrition and Food Science Technology. *Frontiers in Nutrition*, *1*, 4. http://doi.org/10.3389/fnut.2014.00004

Kopsell, D., & Kopsell, D. (2006). Accumulation and bioavailability of dietary carotenoids in vegetable crops. *Trends in Plant Science, 11*(10), 499-507. doi:10.1016/j.tplants.2006.08.006

Kopsell, D., & Sams, C. (2013). Increases in Shoot Tissue Pigments, Glucosinolates, and Mineral Elements in Sprouting Broccoli after Exposure to Short-duration Blue Light from Light Emitting Diodes. *Journal of the American Society for Horticultural Science, 1*(38), 31-37.

Kopsell, D., Sams, C., & Morrow, R. (2017). Interaction of light quality and fertility on biomass, shoot pigmentation and xanthophyll cycle flux in Chinese kale. *Journal of the Science of Food and Agriculture*,*97*(3), 911-917.

Kretschmer, M. (1978). Temperature and Lettuce Seed Germination. *Acta Horticulturae*, (83), 167–174. doi: 10.17660/actahortic.1978.83.22

Kyriacou, M. C., De Pascale, S., Kyratzis, A., & Rouphael, Y. (2017). Microgreens as a Component of Space Life Support Systems: A Cornucopia of Functional Food. *Frontiers in plant science*, *8*, 1587. doi:10.3389/fpls.2017.01587

Kyriacou, M. C., Rouphael, Y., Gioia, F. D., Kyratzis, A., Serio, F., Renna, M., … Santamaria, P. (2016). Micro-scale vegetable production and the rise of microgreens. *Trends in Food Science & Technology*, *57*, 103–115. doi: 10.1016/j.tifs.2016.09.005

Li, J., Li, G., Wang, H., & Wang Deng, X. (2011). Phytochrome signaling mechanisms. *The arabidopsis book, 9*, e0148. doi:10.1199/tab.0148

Liu, R. H. (2004). Potential Synergy of Phytochemicals in Cancer Prevention: Mechanism of Action. *The Journal of Nutrition*, *134*(12). doi: 10.1093/jn/134.12.3479s

Martins, V. J., Florêncio, T. M., Grillo, L. P., Franco, M. D., Martins, P. A., Clemente, A. P., Sawaya, A. L. (2011). Long-Lasting Effects of Undernutrition. *International Journal of Environmental Research and Public Health,8*(12), 1817-1846. doi:10.3390/ijerph8061817

Mccree, K. (1971). The action spectrum, absorptance and quantum yield of photosynthesis in crop plants. *Agricultural Meteorology*, *9*, 191–216. doi: 10.1016/0002-1571(71)90022-7

Metallo, Rosalie M., "The Impact of Genetic and Environmental Factors on Phytonutrient Concentrations within Leafy Specialty Crops in Controlled Environments. " Master's Thesis, University of Tennessee, 2017. https://trace.tennessee.edu/utk_gradthes/4893

Myers, E. F., Khoo, C., Murphy, W., Steiber, A., & Agarwal, S. (2013). A Critical Assessment of Research Needs Identified by the Dietary Guidelines Committees from 1980 to 2010.*Journal of the Academy of Nutrition and Dietetics,113*(7). doi:10.1016/j.jand.2013.03.023

Naber, T. H., Schermer, T., Bree, A. D., Nusteling, K., Eggink, L., Kruimel, J. W., Katan, M. B. (1997). Prevalence of malnutrition in nonsurgical hospitalized patients and its association with disease complications. *The American Journal of Clinical Nutrition,66*(5), 1232-1239. doi:10.1093/ajcn/66.5.1232

National Cancer Institute. (2011). Usual dietary intakes: food intakes, US population, 2007–10. Available at http://appliedresearch.cancer.gov/diet/usualintakes/pop/2007-10

Nelson JA, Bugbee B (2014) Economic Analysis of Greenhouse Lighting: Light Emitting Diodes vs. High Intensity Discharge Fixtures. PLoS ONE 9(6): e99010. https://doi.org/10.1371/journal.pone.0099010

Nuss, E. T., & Tanumihardjo, S. A. (2011). Quality Protein Maize for Africa: Closing the Protein Inadequacy Gap in Vulnerable Populations. *Advances in Nutrition*, *2*(3), 217–224. doi: 10.3945/an.110.000182

Nutrition Support for Adults: Oral Nutrition Support, Enteral Tube Feeding and Parenteral Nutrition. (2006). National Collaborating Centre for Acute Care (UK).

Onis, M., D. Blössner, M., & Borghi, E. (2011). Prevalence and trends of stunting among pre-school children, 1990–2020. *Public Health Nutrition,15*(01), 142-148. doi:10.1017/s1368980011001315

Ramankutty, N., A. T. Evan, C. Monfreda, and J. A. Foley (2008), Farming the planet: 1. Geographic distribution of global agricultural lands in the year 2000, Global Biogeochem. Cycles, 22, GB1003, doi:10.1029/2007GB002952.

Resh, H. M. (2012). Hydroponic food production : A definitive guidebook for the advanced home gardener and the commercial hydroponic grower. Retrieved from http://ebookcentral.proquest.com

Runkle, E. (2016). *A closer look at far-red radiation - Floriculture*. Retrieved from https://www.canr.msu.edu/resources/far-red-radiation

Samuolienė, G., Viršilė, A., Brazaitytė, A., Jankauskienė, J., Sakalauskienė, S., Vaštakaitė, V.Duchovskis, P. (2017). Blue light dosage affects carotenoids and tocopherols in microgreens. *Food Chemistry, 228*, 50-56. doi:10.1016/j.foodchem.2017.01.144

Semilla Nueva (Ed.). (2017). *Semilla Nueva Annual Report 2017*. Retrieved from https://www.semillanueva.org/wp-content/uploads/2017/07/Semilla-Nueva-Annual-Report_low-res1.pdf

Singh, D., Basu, C., Meinhardt-Wollweber, M., & Roth, B. (2015). LEDs for energy efficient greenhouse lighting. *Renewable and Sustainable Energy Reviews, 49*, 139–147. doi: 10.1016/j.rser.2015.04.117

Stapleton, A. E. (1992). Ultraviolet Radiation and Plants: Burning Questions. *The Plant Cell,4*(11), 1353. doi:10.2307/3869507

Szymanska, R., & Slezak, I. (2017). Physiological and biochemical responses to high light and temperature stress in plants. *Environmental and Experimental Botany,139*, 165-177.

Taiz, L., Zeiger, E., Møller, I. M., & Murphy, A. S. (2015). *Plant physiology and development*. Sunderland, MA: Sinauer Associates,.

Tarquis, A. M., & Bradford, K. J. (1992). Prehydration and Priming Treatments that Advance Germination also Increase the Rate of Deterioration of Lettuce Seeds. *Journal of Experimental Botany, 43*(3), 307–317. doi: 10.1093/jxb/43.3.307

Treadwell, D., & Hochmuth, R. (2017). Microgreens: A New Specialty Crop - University of - EDIS.

United States Department of Agriculture. (2010). 2010 Dietary Guidelines - health.gov. Retrieved from https://health.gov/dietaryguidelines/2010/

United States Energy Department. (2019). LED Lighting. Retrieved from https://www.energy.gov/energysaver/save-electricity-and-fuel/lighting-choices-save-you-money/led-lighting

USDA National Nutrient Database for Standard Reference. (2011). Release 24; http://www.ars.usda.gov/nutrientdata

Walker, S., Wachs, T., & Gardner, J. (2007). Child development: risk factors for adverse outcomes in developing countries. *Child: Care, Health and Development*,*33*(4), 502-502. doi:10.1111/j.1365-2214.2007.00774_2.x

White, A. L., & Jahnke, L. S. (2002). Contrasting Effects of UV-A and UV-B on Photosynthesis and Photoprotection of β-carotene in two Dunaliella spp. *Plant and Cell Physiology*,*43*(8), 877-884. doi:10.1093/pcp/pcf105

Willett, W. C. (1995). Diet, Nutrition, and Avoidable Cancer. *Environmental Health Perspectives*, *103*, 165. doi: 10.2307/3432305

Willett, W. C. (2002). Balancing Life-S tyle and Genomics Research for Disease Prevention. *Science*, *296*(5568), 695–698. doi: 10.1126/science.1071055

Xiao, Z., Bauchan, G., Nichols-Russell, L., Luo, Y., Wang, Q., & Nou, X. (2015). Proliferation of Escherichia coli O157:H7 in Soil-Substitute and Hydroponic Microgreen Production Systems. *Journal of Food Protection*, *78*(10), 1785–1790. doi: 10.4315/0362-028x.jfp-15-063

Xiao, Z., Lester, G. E., Luo, Y., & Wang, Q. (2012). Assessment of Vitamin and Carotenoid Concentrations of Emerging Food Products: Edible Microgreens. *Journal of Agricultural and Food Chemistry*,*60*(31), 7644-7651. doi:10.1021/jf300459b

Yang, D., Kanae, S., Oki, T., Koike, T., & Musiake, K. (2003). Global potential soil erosion with reference to land use and climate changes. *Hydrological Processes*, *17*(14), 2913–2928. doi: 10.1002/hyp.1441

APPENDIX

The photosynthetic photon flux density by wavelength and spectral composition is shown at larger scale for the narrow-band LED light treatments. All PPDF measurements were taken under the light assemblies using an Assensetek© Lighting Passport Spectrometer. Figure A.1 illustrates the spectral photosynthetic photon flux density for the broad-spectrum control.

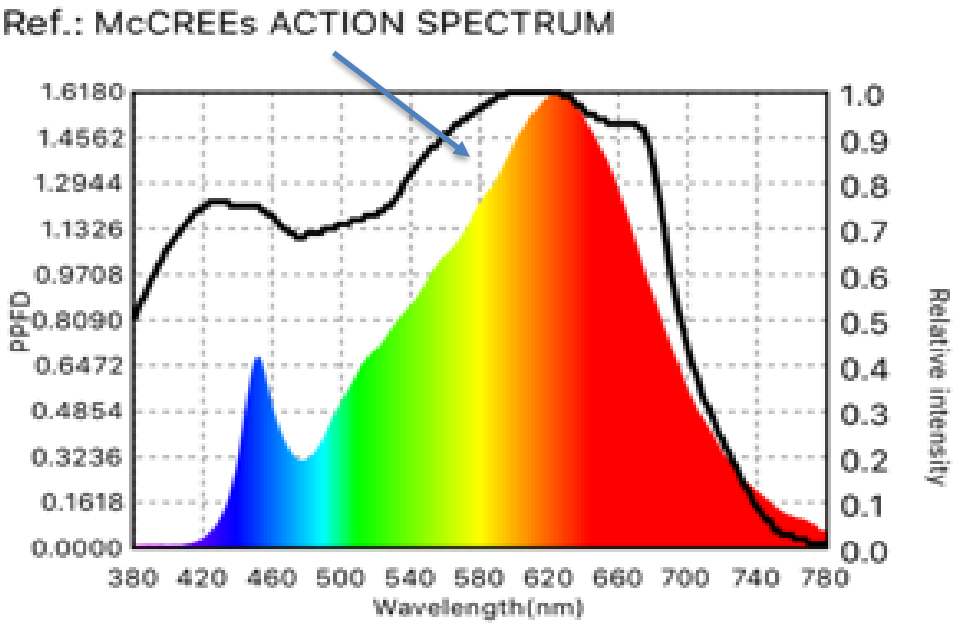


Figure A.1 Photosynthetic photon flux density (μmol·m^{-2}·s^{-1} PAR) by wavelength for the broad-spectrum white LED control group.

Relative intensity is shown respective to the most intense wavelength. McCree's quantum efficiency curve is drawn in black, showing the absorption efficiency of chlorophyll to various wavelengths of light. Figure A.2 illustrates the spectral photosynthetic photon flux density for the infrared supplementation group. The photosynthetic photon flux density by wavelength is shown for the red supplementation group in Figure A.3. McCree's (1971) work gives us some idea that light in the 650-700 nm region is mostly absorbed by chlorophyll in conducting photosynthesis. The peak wavelength was selected at 660 nm to promote a high rate of photosynthesis based on its accepted quantum absorption levels in plant leaf tissue.

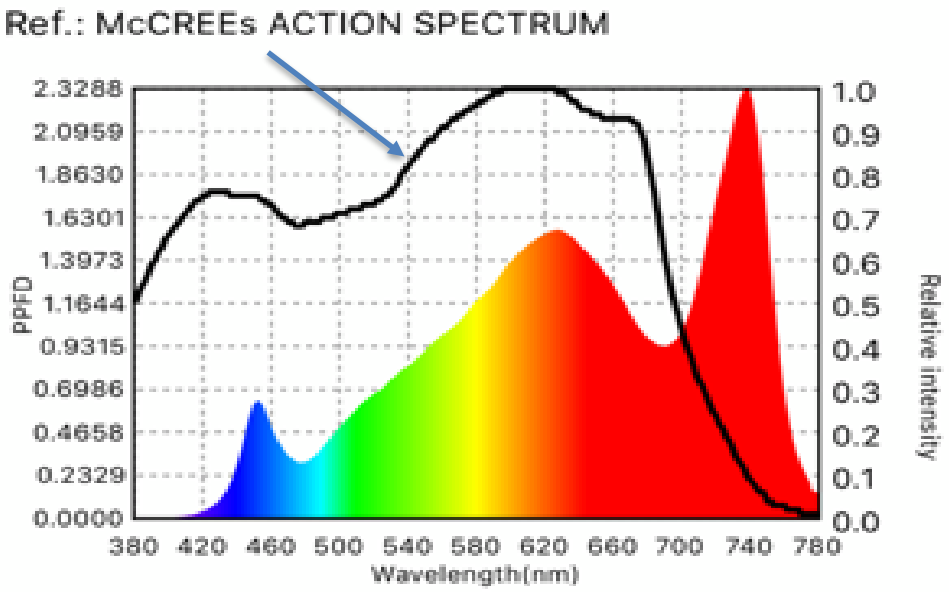


Figure A.2 Photosynthetic photon flux density (μmol·m^{-2}·s^{-1} PAR) by wavelength for the 99% white + infrared supplementation group. Relative intensity is shown respective to the most intense wavelength.

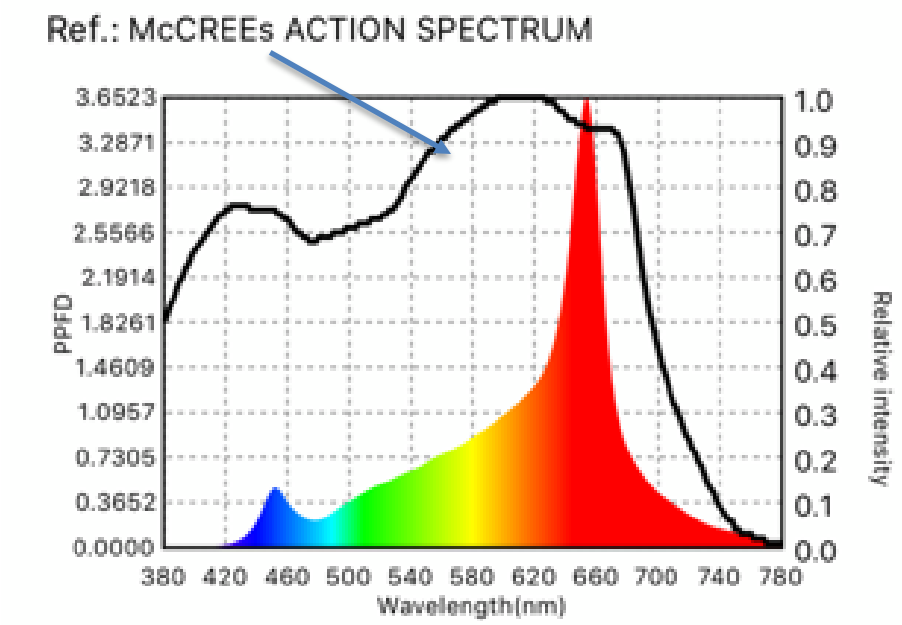


Figure A.3 Photosynthetic photon flux density (μmol·m^{-2}·s^{-1} PAR) by wavelength for the 40% white + red supplementation group. Relative intensity is shown respective to the most intense wavelength. Following the methods of Kopsell et al. (2017), the narrow-band blue supplementation group had its peak wavelength (d) selected at 450 nm to promote increased metabolite content.

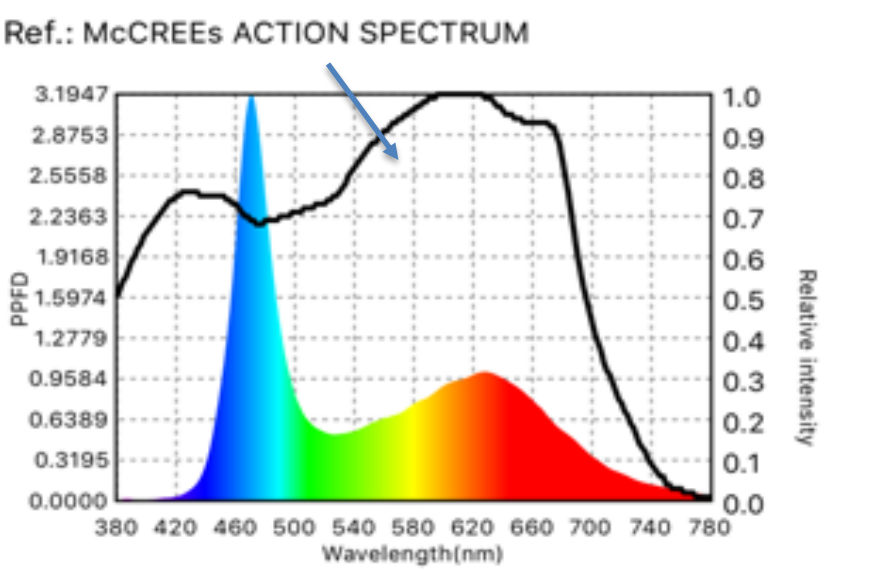


Figure A.4 Photosynthetic photon flux density (μmol·m^{-2}·s^{-1} PAR) by wavelength for the 40% white + blue supplementation group. Relative intensity is shown respective to the most intense wavelength.

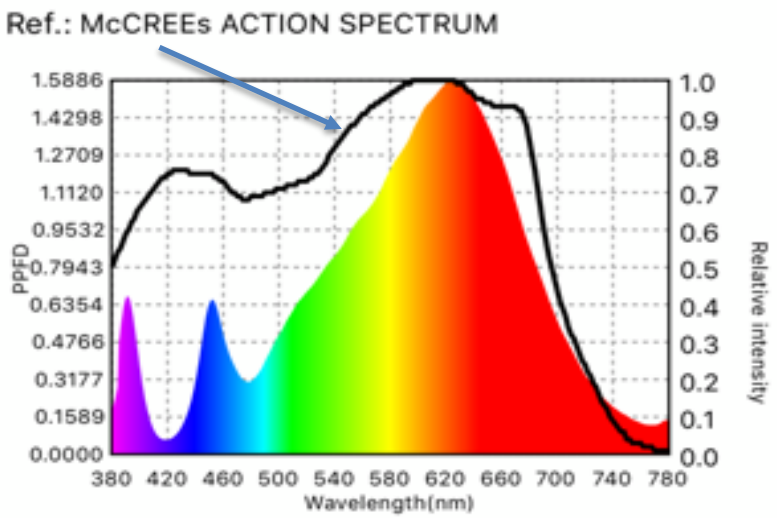


Figure A.5 Photosynthetic photon flux density (μmol·m^{-2}·s^{-1} PAR) by wavelength for the 99% white + ultraviolet supplementation group. Relative intensity is shown respective to the most intense wavelength.

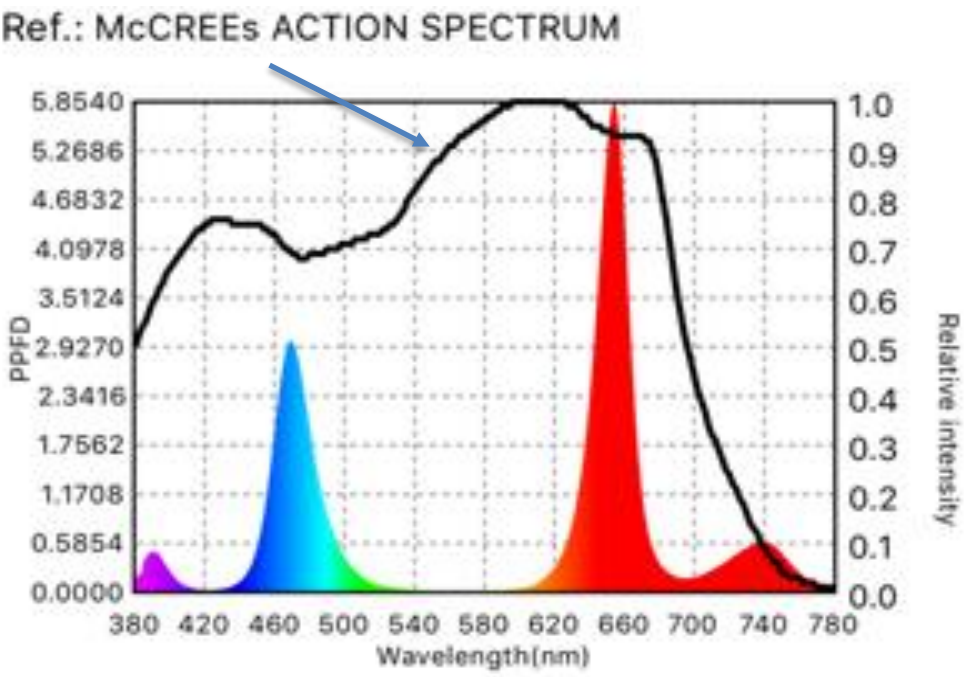


Figure A.6 Photosynthetic photon flux density (μmol·m^{-2}·s^{-1} PAR) by wavelength for the narrow-band isolated spectrum (400, 450, 660, 740 nm) group. Relative intensity is shown respective to the most intense wavelength.

VITA

Colin Brice was born in Plano, TX, but spent most of his youth growing up south of Nashville, TN. After developing a passion for plants, he studied plant sciences at the University of Tennessee, where he was awarded an internship building a microgreen production system in Guatemala. His exposure to a new culture and food system helped him focus this research on the effects of LED light wavelengths and hydroponic system design on microgreen production. He hopes to develop his production and engineering knowledge into methods of producing healthier foods with less resources. Colin will always continue his passion for science and research, whether in commercial or academic settings.